ANKARA UNIVERSITY FACULTY OF PHARMACY

ISOPS 13th International SYMPOSIUM ON PHARMACEUTICAL SCIENCES

Poster no	Presenter	Title	Topic
B1	Miyase Gözde Gündüz	1,4-DIHYDROPYRIDINE-AZOLE HYBRIDS: SYNTHESIS, COMPUTATIONAL STUDIES AND ANTIMICROBIAL ACTIVITY	Pharmaceutical Chemistry
B2	Miyase Gözde Gündüz	SYNTHESIS OF DIHYDROPYRIMIDINE DERIVATIVES WITH L-/T-TYPE CALCIUM CHANNEL BLOCKING ACTIVITIES	Pharmaceutical Chemistry
B3	Dilara Akman	FOCUSING ON C-4 POSITION OF 1,4-DIHYDROPYRIDINE RING: SYNTHESIS AND L-/T-TYPE CALCIUM CHANNEL BLOCKING ACTIVITY	Pharmaceutical Chemistry
B4	Mehmet Murat Kışla	INDOLE-BENZIMIDAZOLE DERIVATIVES AS ANTIBACTERIAL AGENTS AGAINST HOSPITAL INFECTIONS AND THEIR DOCKING PROFILES	Pharmaceutical Chemistry
B5	Fatıma Doğanç	PREPARATION OF SOME PURINE DERIVATIVES: USE OF THE 2D NMR 1H,15N & 1H,13C HMBC TECHNIQUES AND X-RAY CRYSTALLOGRAPHY IN ASSIGNING REGIOCHEMISTRY	Pharmaceutical Chemistry
B6	Muhammed İhsan Han	DESIGN, SYNTHESIS AND ANTIMICROBIAL EVALUATION OF NOVEL ISOQUINOLIN-UREA HYBRIDE MOLECULES	Pharmaceutical Chemistry
B7	Debora Procopio	DEEP EUTECTIC SOLVENTS AS POWERFUL CATALYSTS AND SOLVENTS FOR THE SYNTHESIS OF AMIDES	Pharmaceutical Chemistry
B8	Mevlüt Akdağ	SYNTHESIS OF PLATINUM(II) COMPLEXES WITH 2-SUBSTITUTED BENZIMIDAZOLE LIGANDS	Pharmaceutical Chemistry
B9	Hande Cevher Koç	SYNTHESIS AND ANTICANCER ACTIVITY OF ETODOLAC HYDRAZONES	Pharmaceutical Chemistry
B10	Gözde Yenice Çakmak	SYNTHESIS AND MOLECULAR MODELING STUDIES OF SOME NOVEL BENZOTIAZOLE DERIVATIVES AS ANTI-CANCER AGENTS	Pharmaceutical Chemistry
B11	Belbekiri Habiba	A MONTMORILLONITE CLAY AS AN EFFICIENT AND GREEN CATALYST FOR FUNCTIONAL POLYETHER SYNTHESIS	Pharmaceutical Chemistry
B12	Shakıla Shakıla	SYNTHESIS OF SOME NEW 2-PHENOXYACETAMIDE AND 3-PHENOXYPROPANAMIDE DERIVATIVES AND EVALUATION OF THEIR CHOLINESTERASE INHIBITOR ACTIVITIES	Pharmaceutical Chemistry
B13	Memmou Faiza	SYNTHESIS AND IN VITRO EVALUATION OF THE ANTIOXIDANT ACTIVITY OF IMINES	Pharmaceutical Chemistry
B14	Caner Arıkan	SYNTHESIS AND STANDARDIZATION OF AN IMPURITY OF ACETAMINOPHEN, DEVELOPMENT AND VALIDATION OF RELATED ULTRA-HIGH PERFORMANCE LIQUID CHROMATOGRAPHIC METHOD	Pharmaceutical Chemistry
B15	Serap İpek Dingiş Birgül	IN SILICO DESIGN AND SYNTHESIS OF NOVEL 2-ACYLHYDRAZONO-5-ARYLMETHYLENE-4-THIAZOLIDINONES AS ENOYL-ACYL CARRIER PROTEIN REDUCTASE INHIBITORS	Pharmaceutical Chemistry

1,4-DIHYDROPYRIDINE-AZOLE HYBRIDS: SYNTHESIS, COMPUTATIONAL STUDIES AND ANTIMICROBIAL ACTIVITY

Miyase Gözde Gündüz[a], Cagatay Dengiz[b], Ebru Koçak Aslan[a], Sanja Skaro Bogojevic[c], Jasmina Nikodinovic-Runic[c]

[a]Department of Pharmaceutical Chemistry, Faculty of Pharmacy, Hacettepe University, Sıhhiye, 06100, Ankara, Turkey, miyasegunduz@yahoo.com

[b]Department of Chemistry, Middle East Technical University, 06800, Ankara, Turkey

[c]Institute of Molecular Genetics and Genetic Engineering, University of Belgrade, Vojvode Stepe 444a, 11000 Belgrade, Serbia

INTRODUCTION

Heterocyclic compounds hold a significant position not only in organic but also in medicinal chemistry, especially during the drug design process [1]. Among various heterocycles, nitrogen-containing scaffolds attract great interest due to their wide range of pharmacological properties and are frequent structural motifs of therapeutically valuable compounds [2]. 1,4-dihydropyridine (DHP) is the most famous isomer playing key role in synthetic and medicinal chemistry [3]. Azoles are five-membered nitrogen-containing heterocycles carrying at least one more heteroatom such as nitrogen, oxygen or sulfur as the component of the ring. Although they possess a broad spectrum of promising biological profiles, imidazole and triazole-carrying molecules stand forward with their antifungal activities [4]. In this study, we aimed to combine two precious rings, 1,4-dihydropyridine and azoles, in the same molecule.

MATERIAL and METHODS

4-Azolyl benzaldehydes were synthesized through the nucleophilic aromatic substitutions of 4-fluorobenzladehyde with different azoles (pyrazole, imidazole or 1,2,4-triazole). Subsequently, DHPs were obtained according to modified Hantzsch synthesis. Antibacterial and antifungal activities of the compounds were evaluated according to the standard broth micro-dilution assays. Molecular docking studies were carried out using AutoDock in the binding site of *Candida albicans* lanosterol 14α-demethylase (CYP51). Furthermore, optoelectronic properties of the hybrid structures were investigated by computational studies (TD-DFT, electrostatic potential maps, HOMO-LUMO orbital depictions) using Gaussian 09 program package.

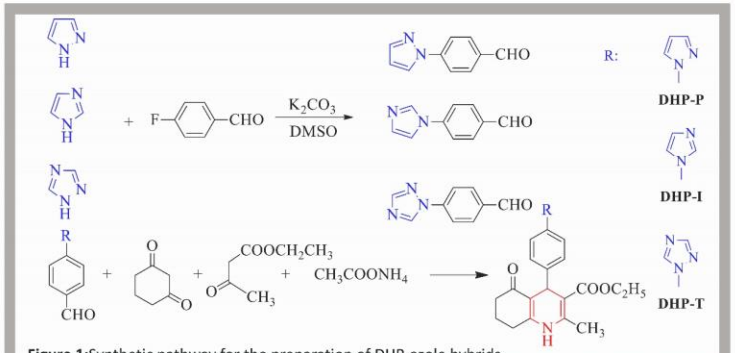

Figure 1: Synthetic pathway for the preparation of DHP-azole hybrids.

RESULTS

* DHP-azole hybrids demonstrated moderate antifungal activities against *Candida* strains.

Table 1. Antimicrobial activity (MIC values µg/mL) of DHP-azole hybrids on different *Candida* species

Organisms	DHP-P	DHP-I	DHP-T
Candida albicans ATCC 10231	500	250	250
Candida parapsilosis ATCC 22019	> 500	250	250
Candida krusei ATCC 625	500	>500	>500
Candida glabrata ATCC 2001	>500	500	250

* To estimate the drug-likeness of the synthesized compounds, we calculated Lipinski's rule of five.

Table 1. Calculated molecular properties of DHP-azole hybrids

Compound	MW[a]	LogP[b]	HBD[c]	HBA[d]	NRB[e]	TPSA[f]	Lipinski's Violation
DHP-P	377.44	2.84	1	4	5	73.22	0
DHP-I	377.44	2.72	1	4	5	73.22	0
DHP-T	378.42	2.49	1	5	5	86.11	0

[a]M.W: molecular weight
[b]LogP: logarithm of *n*-octanol-water partition coefficient
[c]HBA: number of hydrogen bond acceptors
[d]HBD: number of hydrogen bond donors
[e]NRB: number of rotatable bonds
[f]TPSA: topological polar surface area

* In molecular docking studies, we observed that azole rings could not make the essential interaction through the coordination of the nitrogen atom with the iron of heme in the active site of CYP51.

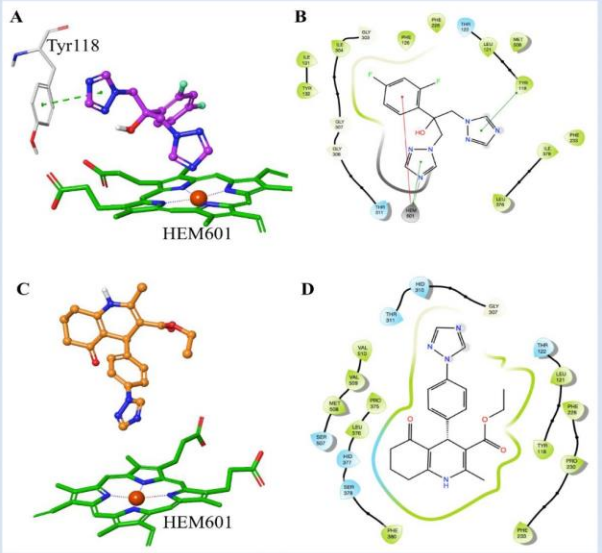

Figure 2. Proposed binding modes of fluconazole (A) and **DHP-T** (C) in the catalytic site of *Candida albicans* CYP51, and their 2D interaction diagrams (B and D, respectively). Fluconazole and **DHP-T** are represented as purple and orange ball&stick, respectively. Heme and heme iron are shown as green stick and orange CPK.

*HOMO and LUMO visualizations revealed that azole-substituents have almost no impact on CT properties of DHP-azole hybrids . While LUMO centered around electron-deficient carbonyl groups, it is demonstrated that HOMOs are delocalized around nitrogen containing region with almost no support from azole rings.

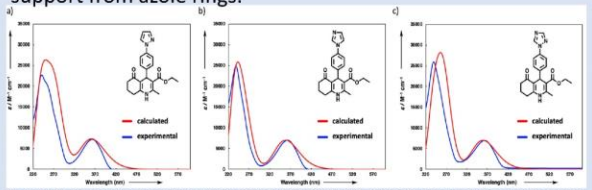

Figure 3: Calculated (red line) TD-DFT:CAM-B3LYP/6–31G(d) level of theory in EtOH and experimental UV/Vis spectrum of synthesized compounds in EtOH (blue line)

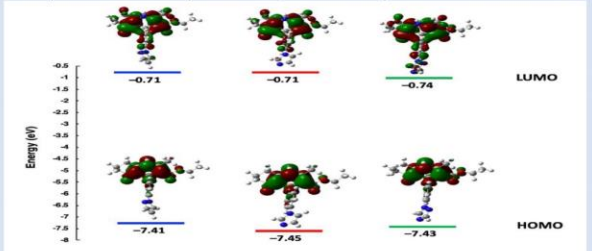

Figure 4: Energy level diagram of the HOMO and LUMO of synthesized compounds estimated by DFT calculations

*Electrostatic potential maps were also utilized as they can provide qualitative proof for CT properties of DHP-azole hybrids.

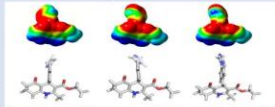

Figure 5: ESP maps of DHP-azole hybrids.

CONCLUSIONS

*In this study, we report the synthesis of DHP-azole hybrids carrying azoles directly attached to the phenyl ring at C-4 position of DHP scaffold. Molecular docking studies suggested that providing flexibility to the azole ring can lead to more active antifungal agents.

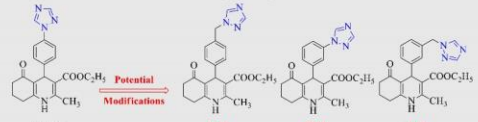

Figure 5: Suggested possible molecular modifications on **DHP-T** with the aim of obtaining active antifungals

*Consequently, carrying the triazole ring from C-4 to C-3 phenyl ring directly or with a methylene bridge led to the potential antifungal DHP-azole hybrids. These results, obtained through molecular docking studies, should be confirmed by biological assays after the synthesis of the suggested compounds.

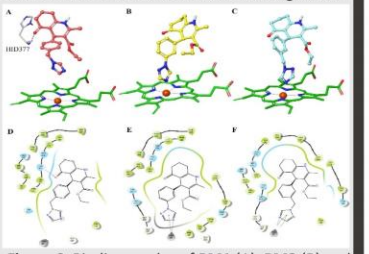

Figure 6. Binding modes of **PM1** (A), **PM2** (B) and **PM3** (C), and 2D depiction of ligand-enzyme interactions for **PM1** (D), **PM2** (E) and **PM3** (F) in the active site of *Candida albicans* CYP51. Ligands are represented as pink, yellow and cyan ball&sticks for **PM1**, **PM2** and **PM3**, respectively. Heme and heme iron are shown as green stick and orange CPK.

References

1. Taylor A.P., et al. (2016). Org Biomol Chem, 14: 6611–6637. **3.** SharmaV.K. et al. (2017). RSC Adv. 7: 2682–2732
2. Kerru et al. (2020). Molecules, 25: 1909. **4.** Shafiei M. et al. (2020). Bioorg. Chem. 104: 104240

SYNTHESIS OF DIHYDROPYRIMIDINE DERIVATIVES WITH L-/T-TYPE CALCIUM CHANNEL BLOCKING ACTIVITIES

Miyase Gözde Gündüz[a], Cagatay Dengiz[b], Sun Huang[c], Gerald W. Zamponi[c]

[a]Department of Pharmaceutical Chemistry, Faculty of Pharmacy, Hacettepe University, Sıhhiye, 06100, Ankara, Turkey, miyasegunduz@yahoo.com

[b]Department of Chemistry, Middle East Technical University, 06800, Ankara, Turkey

[c]University of Calgary, Hotchkiss Brain Institute and Alberta Children's Hospital Research Institute, Department of Physiology and Pharmacology, Calgary, Canada

INTRODUCTION

Calcium channel blockers act by blocking the entry of calcium ion into the cells through specific channels. 1,4-Dihydropyridines (DHPs) are the most famous group of commercial calcium channel blockers that are used for the treatment of hypertension through blocking L-type calcium channel (1). Recent studies showed that DHPs can also target T-type calcium channel isoforms that are associated with neurological disorders, hence they are considered as druggable targets for the treatment of neurophysiologic conditions, particularly epilepsy and pain (2). Dihydropyrimidine (DHPM) ring is the classical bioisostere of DHP and is expected to mediate similar pharmacological activities (3). In light of these considerations, we aimed to synthesize DHPM derivatives by changing the ester group and substituents on the phenyl ring. The synthesized compounds were tested as blockers of CaV1.2 and CaV3.2 using the whole-cell patch clamp technique.

MATERIAL and METHODS

DHPM derivatives were obtained by the reaction of isobutyl/benzyl acetoacetates, substituted benzaldehydes (3-nitrobenzaldehyde/5-nitrosalicylaldehyde/5-bromo-3-methoxysalicylaldehyde), and urea in ethanol. Subsequently, N3 position and the phenolic hydroxyl group of the obtained compounds were acetylated via heating in acetic anhydride. Calcium channel blocking effects of these compounds were determined on L-type (Cav1.2) and T-type (Cav3.2) calcium channels by patch-clamp assays.

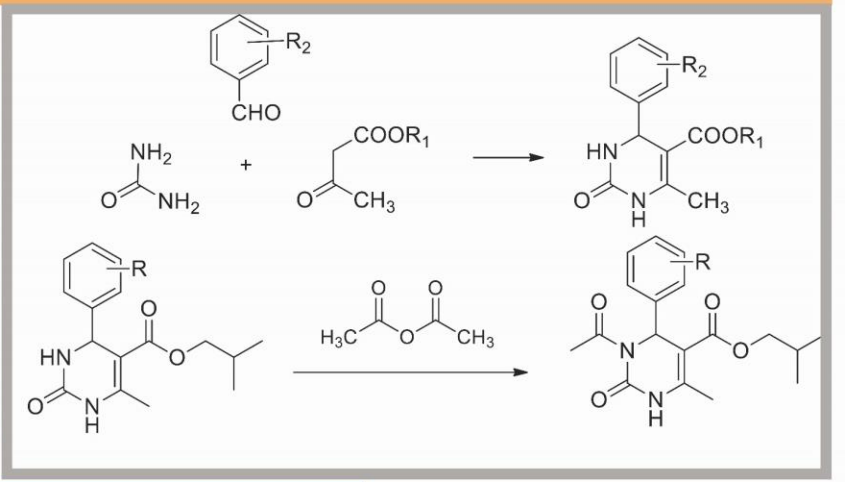

RESULTS and DISCUSSION

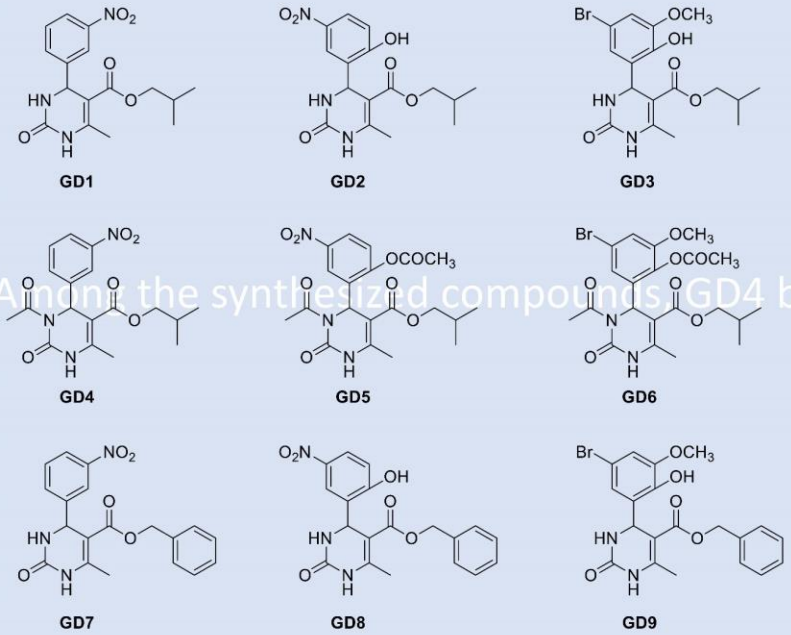

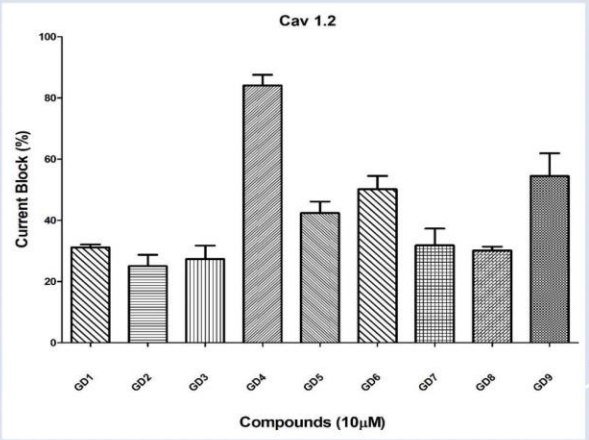

Among the synthesized compounds, **GD4** blocked both calcium channels subtypes effectively.

Introducing acetyl group to the structures of the compounds resulted in increased L-type calcium channel blocking activity.

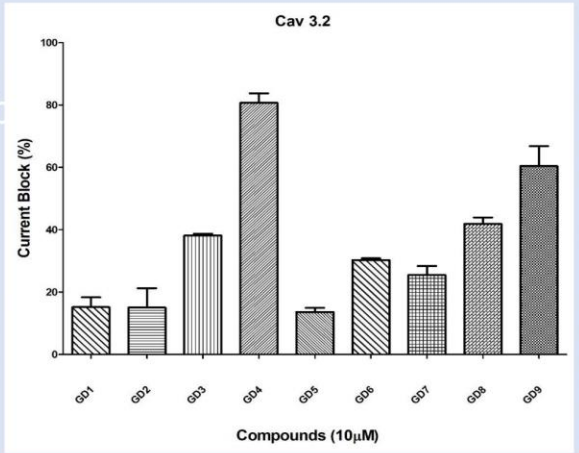

CONCLUSIONS

In this study, we synthesized and identified new DHPM-based calcium channel blockers which hold therapeutic value in the treatment of cardiovascular and neurological diseases.

REFERENCES

1. Zamponi GW, Striessnig J, Koschak A, Dolphin AC (2015). Pharmacological Reviews, 67:821-870.
2. Schaller D, Gündüz MG, Zhang FX, Zamponi GW, Wolber G (2018). European Journal of Medicinal Chemistry, 155:1-12.
3. Teleb M, Rizk OH, Zhang FX, Fronczek FR, Zamponi GW, Hesham F (2019). Bioorganic Chemistry, 83:354-366.

FOCUSING ON C-4 POSITION OF 1,4-DIHYDROPYRIDINE RING: SYNTHESIS AND L-/T-TYPE CALCIUM CHANNEL BLOCKING ACTIVITY

[1]Dilara AKMAN,[2]Sun HUANG,[2]Gerald W. ZAMPONI, [1]Miyase Gözde GÜNDÜZ

[1] Hacettepe University, Faculty of Pharmacy, Department of Pharmaceutical Chemistry, Ankara, Turkey, dilaraakman@protonmail.com,

[2]University of Calgary, Hotchkiss Brain Institute and Alberta Children's Hospital Research Institute,Department of Physiology and Pharmacology, Calgary, Canada

Abstract

Voltage gated calcium channels are importartant target for drug development and designing owing to their roles on gene transcription, muscle contraciton, hormon and norotransmitter secretion etc. 1.4-dihydropyridines, known as L-type calcium channel blockers, are mostly used compounds for the treatment of hypertansion and angina. Recently revealed that some of 1,4-dihydropyridines are also blocking T-type calcium channels. In this study, we synthesized twelve different 1,4-dihydropyridine derivates focusing on the modifications of C-4 position. We evaluated the obtained compounds for their L-/T-type calcium channel blocking effects.

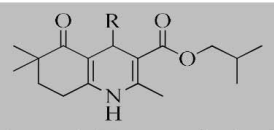

R: Aromatic/Heterocyclic ring/
Phenyl ring with bulky substituent

Introduction

1,4-Dihydropyridines (DHPs), represented by nifedipine and amlodipine, are widely prescribed for the treatment of hypertension (1). Although their primary target in the cardiovascular system is the L-type calcium channel isoform, DHPs can also block low-voltage-activated T-type calcium channels (2). Commercial DHPs generally carry phenyl rings with small substituents at C-4 position. In this study, we aimed to investigate the effects of bulky groups at the mentioned position to the L-/T-type calcium channel blocking activities of DHPs.

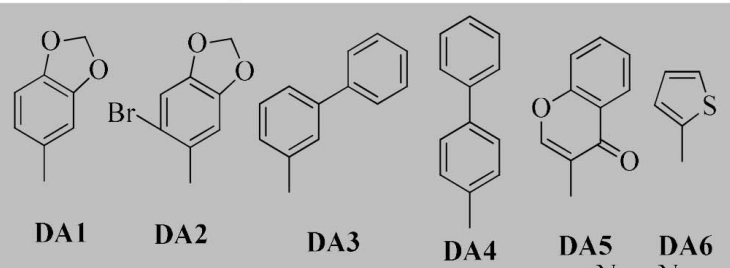

Methodology

Synthesis:

The general procedure for the synthesis of 1,4-DHP derivatives was as follows: 1 mmol 4,4-dimethyl-1,3-cyclohexanedione, 1 mmol aldehyde, 1 mmol isobutyl acetoacetate and excess amount of ammonium acetate were dissolved in a 35-ml microwave pressure vial in absolute ethanol and subjected to microwave irradiation (power 100 W) for 10 min. After completion of the reaction, monitored by TLC, the reaction mixture was cooled, poured into ice-water. The obtained precipitate was filtered and this crude solid was purified by recrystallization from ethanol-water.

Electrophysiology:

Cells on a glass coverslip were transferred into an external bath solution of 20 mM $BaCl_2$, 1 mM $MgCl_2$, 40 mM TEACl, 65 mM CsCl, 10 mM HEPES, and 10 mM glucose, pH 7.4. Borosilicate glass pipettes (Sutter Instrument Co., Novato, CA; pipette resistance of 3–5 MΩ) were filled with internal solution containing 140 mM CsCl, 2.5 mM $CaCl_2$, 1 mM $MgCl_2$, 5 mM EGTA, 10 mM HEPES, 2 mM Na-ATP, and 0.3 mM Na-GTP, pH 7.3. Whole-cell patch clamp recordings were performed by using an EPC 10 amplifier (HEKA Elektronik, Bellmore, NY) coupled to a computer running Pulse (V8.65) software (HEKA Elektronik). After seal formation, cells were dialzyed for 5 min before recording. Voltage-dependent currents were leak corrected with an online P/4 subtraction paradigm. Data were recorded at 10 kHz and filtered at 2.9 kHz. Cav3.2 currents were evoked by depolarization from a holding potential of −110 mV to a test potential of −20 mV and L-type currents were evoked by depolarization from a holding potential of −90 mV to a test potential of +20 mV. The interpulse interval was 20 s, and the test pulse was typically 100 ms long. Data analysis was performed with Pulse software (HEKA Elektronik), and all graphs were prepared by using GraphPad Prism 5 (GraphPad Software, La Jolla, CA).

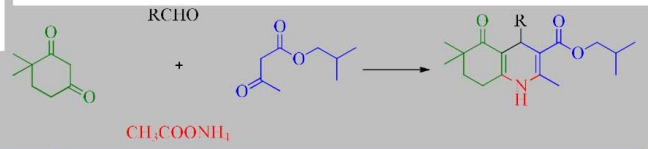

Results

Some of the synthesized compounds effectively blocked L-/T-type calcium channels with different selectivity profiles. 1,3-Benzodioxole ring at C-4 provided the best selectivity on Cav3.2 over Cav1.2.

Various spectral methods (^{1}H-NMR, ^{13}C-NMR and mass spectra) and elemental analysis were carried out to elucidate the structures of the obtained compounds.

The calcium channel blocking activities of the compounds were evaluated on L- and T-type calcium channel using patch-clamp assays.

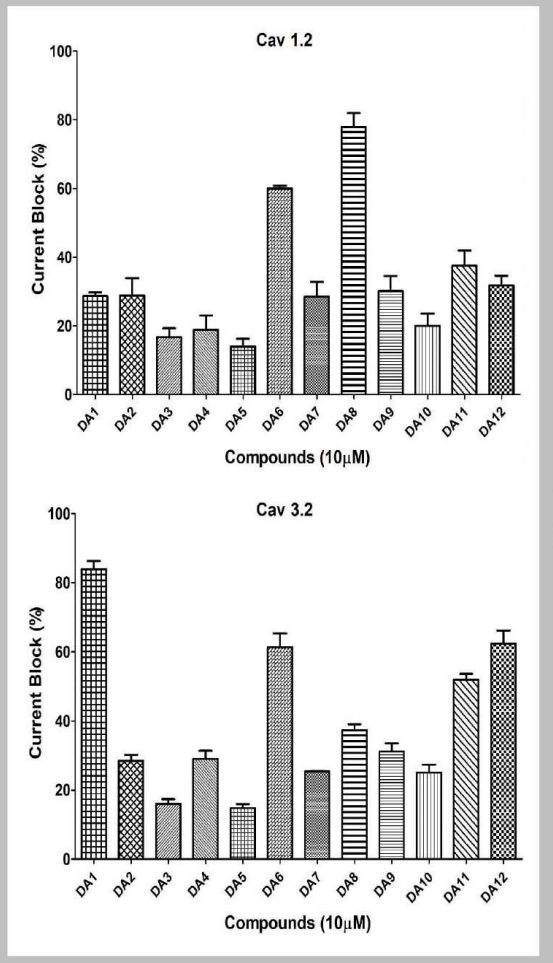

Conclusion

In this study, we synthesized DHPs focusing on the modifications at C-4 position. Introducing different rings rather than phenyl, which is common in commercial DHPs, led to the discovery of effective calcium channel blockers.

Acknowledgements

1. Zamponi GW, Striessnig J, Koschak A, Dolphin AC (2015). Pharmacological Reviews, 67:821-870.
2. Schaller D, Gündüz MG, Zhang FX, Zamponi GW, Wolber G (2018). European Journal of Medicinal Chemistry, 155:1-12.
3. A Crash Course in Calcium Channels Zamponi GW

INDOLE-BENZIMIDAZOLE DERIVATIVES AS ANTIBACTERIAL AGENTS AGAINST HOSPITAL INFECTIONS AND THEIR DOCKING PROFILES

[1]Zengin-Karadayi, F., [1]Kisla, M.M., [2]Kaskatepe, B., [1]Ates-Alagoz, Z.

[1] Ankara University Faculty of Pharmacy, Department of Pharmaceutical Chemistry, Ankara, Turkey, mmkisla@ankara.edu.tr

[2] Ankara University Faculty of Pharmacy, Department of Pharmaceutical Microbiology, Ankara, Turkey, bkaskatepe@ankara.edu.tr

1. INTRODUCTION

Topoisomerase-II DNA-gyrase and Topoisomerase-IV are two types of Topoisomerase-II that regulate cell survival by catalyzing the topological modifications in bacteria cells. These enzymes are also structurally similar heterotetramers and their subunits are defined as GyrA/GyrB for DNA-gyrase and ParC/ParE for Topo-IV. They unlink the DNA by making several cuts with the tyrosine residue at the catalytic site of the enzymes. Mechanistically, gyrase facilitates chain elongation during the chromosome replication whereas Topo-IV acts in final stage of DNA replication and separates the daughter chromosomes that are topologically connected. These different roles of these enzymes are due to their distinct biochemical properties, physiological roles etc. [1]. When the reactions in these control mechanisms for the cellular replication (supercoiling and decatenation) are interrupted, bacterial cells fail to multiply and eventually progress into cell death [2]. Therefore, these enzymes become noteworthy targets for antibacterial drug discovery since they exist in bacteria strains and is absent from eukaryotic cells (3).

Benzimidazole ring is an isostere of purine core in biosystems [4] therefore it can sterically replace these cores inside many biopolymers. The strategy for using different structures that have benzimidazole moiety has become popular in the past years. For instance, Charifson et al. investigated benzimidazole-urea hybrids as dual-targeting inhibitors of DNA gyrase and Topo-IV, In the end they have identified the necessities in SAR for better inhibition of these enzymes [5]. On the other hand, Bansal et al. introduced 3,4-dimethoxyphenyl bis-benzimidazole as a novel DNA topoisomerase inhibitor that is selective against Escherichia coli topoisomerase I [6]. Gullapelli et al. synthesized novel benzimidazole analogues having triazinane and oxadiazinane rings instead of benzene and separated some of them as potent Topo-II DNA gyrase and Topo-IV poisons. Moreover, they have analysed these compounds in silico and the results were consistent with their bioactivity results and binding assays [7].

In line with the above-mentioned studies, we implemented design and synthesis of several novel benzimidazole derivatives fused with indole ring (**1-11**) and probed their antibacterial activity on various bacteria strains. Furthermore, we analyzed the docking results of the most potent compound **3** with DNA-gyrase B subunit and Topoisomerase-IV enzymes and compared them to the standard inhibitor Ciprofloxacin.

2. METHODS

2.1. SYNTHESIS

A mixture of the appropriate *o*-phenylenediamine (1 mmol), indole-3-carboxaldehyde (1 mmol) and $Na_2S_2O_5$ (40%) (2 mL) in EtOH (4 mL) was refluxed until consumption of the starting material (determined by TLC, 4-12 h). The reaction mixture was poured into water, and the precipitate was filtered and washed with water. The residue was purified by column chromatography and crystallized with MeOH to give the final product (**Scheme**).

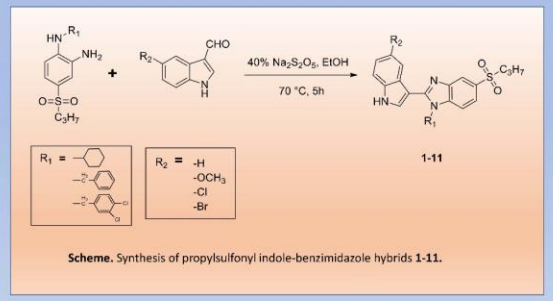

Scheme. Synthesis of propylsulfonyl indole-benzimidazole hybrids **1-11.**

2.2. CHEMISTRY

Melting points were determined and uncorrected using Buchi SMP-20 (BuchiLabortechnik, Flawil, Switzerland) and Electrothermal 9100 capillary melting point apparatus (Electrothermal, Essex, U.K.). The 1H NMR spectra in DMSO-d6 using Varian Mercury-400 FT-NMR spectrometer (Varian Inc., Palo Alto, CA, USA), and the Mass spectra based on ESI(+) method using Waters ZQ micromass LC-MS spectrometer (Waters Corporation, Milford, MA, USA) were measured. For elemental analysis and column chromatography (cc), respectively, LECO 932 CHNS (Leco-932, St. Joseph, MI, USA) instrument and Silica gel 60 (40–63 mm particle size) were used. 1-chloro-4-(propylsulfonyl)benzene and indole-3-carboxaldehyde were obtained commercially. The 5-substituted-indole-3-carboxaldehyde derivatives were obtained by direct formylation of 5-substituted-indole with dimethylformamide, using phosphorous oxychloride as a catalyst [8].

2.3. ANTIMICROBIAL ACTIVITY

The antimicrobial activity of compounds were determined against *Escherichia coli* ATCC 25922, *Pseudomonas aeruginosa* ATCC 9027, *Acinetobacter baumannii* ATCC 19606, *Klebsiella pneumonia* ATCC 18883, *Staphylococcus aureus* ATCC 29213, Methicillin Resistant *Staphylococcus aureus* (MRSA) ATCC 43300, *Enterococcus faecalis ATCC* 29212 with using micro-dilution method [9]. For this purpose, double-fold dilutions were prepared by adding 100 µL of sample to the first well of the microplate containing 100 µL of Cation adjusted Mueller Hinton Broth (Becton Dickinson) in each well. Then, bacterial suspensions, prepared from fresh bacterial cultures and equal to McFarland 0.5 turbidity, were diluted at a ratio 1/100 and 100 µL was added to all wells. Microplates were incubated at 37°C for 16-20 hours. The lowest concentration that inhibit the bacterial growth was determined as the Minimal Inhibition Concentration (MIC).

2.3. MOLECULAR DOCKING ANALYSIS

Structure files for DNA gyrase B subunit (pdb id: 3ttz) and Topoisomerase-IV ParE subunit (pdb id: 4url) were obtained from the RCSB Protein database website [10]. AutoDockTools 1.5.6. was used for deleting water molecules and defining the grid box [11]. After this process, polar hydrogens and Gasteiger charges were added, and the grid was also prepared using the same software. The 2D structures of the compounds were drawn on ChemDraw Ultra 12.0, minimized with MMFF94 and UFF forcefields to achieve the lowest energy conformer of the compounds. After the minimization process, these files were converted to pdb files using Avogadro software [12]. Subsequently, Gasteiger charges and torsion were added to ligand files with AutoDockTools. Prepared ligands were docked with Autodock Vina, [13] interaction diagrams, were created and interpreted using Discovery Studio Visualizer Ligand interaction module [14].

3. RESULTS

3.1. BIOLOGICAL ACTIVITY

Antibacterial activity of the standard **CIP** and standards **1-11** were probed against several strains including *Escherichia coli* ATCC 25922, *Pseudomonas aeruginosa* ATCC 9027, *Acinetobacter baumannii* ATCC 19606, *Klebsiella pneumonia* ATCC 18883, *Staphylococcus aureus* ATCC *29213,* MRSA* ATCC 43300, and *Enterococcus faecalis* ATCC *29212* respectively. According to the results obtained, all the compounds have had high inhibitory effect on Gram positive strains. For instance, compound **3** had MIC value of 0.48 µg/mL on *Staphylococcus aureus* ATCC 29213 strain. This value was 31.2 µg/mL for MRSA ATCC 43300 and 62.5 for *Enterococcus faecalis ATCC* 29212, proving that this compound was selective for *S. aureus*. MIC value of Ciprofloxacin was 0.25 µg/mL for *Staphylococcus aureus* ATCC 29213 (**Table 1**). This data has given us a prominent antibacterial lead that we will analyze against both cell survival enzymes in bacteria.

Table 1. The antibacterial activity results of compounds (µg/mL)

Samples	*Escherichia coli* ATCC 25922	*Pseudomonas aeruginosa* ATCC 9027	*Acinetobacter baumannii* ATCC 19606	*Klebsiella pneumonia* ATCC 18883	*Staphylococcus aureus* ATCC *29213*	MRSA* ATCC 43300	*Enterococcus faecalis* ATCC *29212*
CIP*	0.0078	nt*	nt	nt	0.25	nt	0.5
1	>250	>250	>250	>250	62.5	31.2	31.2
2	>250	>250	>250	>250	7.8	125	31.2
3	>250	>250	>250	>250	0.48	31.2	62.5
4	>250	>250	>250	>250	62.5	62.5	62.5
5	>250	>250	>250	>250	62.5	62.5	62.5
6	>250	>250	>250	>250	125	62.5	62.5
7	>250	>250	>250	>250	125	125	31.2
8	>250	>250	>250	>250	125	62.5	31.2
9	>250	>250	>250	>250	62.5	62.5	31.2
10	>250	>250	>250	>250	125	125	31.2
11	>250	>250	>250	>250	62.5	62.5	62.5

* CIP: Ciprofloxacin; MRSA: Methicillin Resistant *Staphylococcus aureus*; nt: not tested.

3.2. MOLECULAR DOCKING

According to the MIC assay, compound **3** was elected as the potent compound, and compared to the standard **Ciprofloxacin** in docking analysis. Binding pose and interactions of this ligand with DNA-gyrase and Topoisomerase-IV was taken as baseline for comparative analysis. Docked pose of these ligands were given in **Figure 1.**

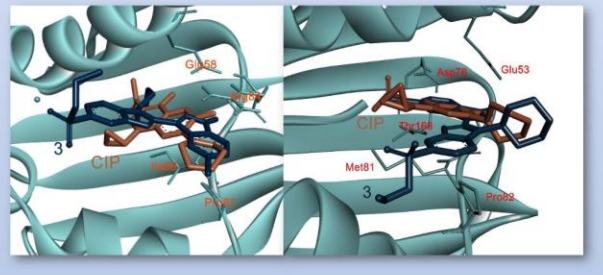

A B

Figure 1. 3D docked poses for the ligands **CIP** and **3** at the binding regions of DNA gyrase B-subunit (**A**) and Topo-IV ParE subunit (**B**). Interacting residues for **CIP** were also highlighted for reference.

For the docking with DNA-gyrase, aromatic residues facilitate the pi-stacking with Arg84 and groups such as carboxylate or carboxamide form H-bond interactions with Arg144 and Asp81 [15].Our docking results with **CIP** were much like this profile, giving other H-bond interactions with Ser55, Thr173, Arg84 and fundamental Asp81 (**Figure 2A**). After this, docking interactions and binding energy of the compound **3** were analyzed. For this compound, benzimidazole and indole rings were responsible for numerous hydrophobic interactions such as Ile102, Ala61, and Asp57. In addition, like the cyclopropyl group that is present in **CIP**, this compound offered cyclohexyl group for an interaction with Ile86. Indole nitrogen offered H-bond interactions with Glu58 and Asp57 (**Figure 2B**).

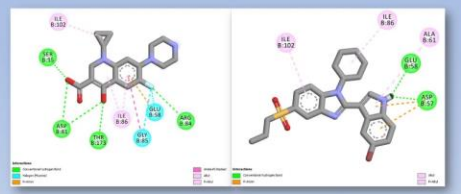

A B

Figure 2. Interacting residues of DNA-gyrase B subunit with **CIP** (**A**) and compound **3** (**B**)

For the dual inhibition by our indole-benzimidazole derivatives, docking results with Staph Topo-IV ParE subunit were also studied. The important residues were hydrophobic residues such as Ile46, Ile175, Val79, and polar residues such as Glu58, His86, and Gly109 [16]. Herein, we have docked **CIP** with Pare to witness the pattern-wise similarities. This ligand offered lesser interactions consisting of some common residues such as Met81 and Glu53, and additional H-bonds via -OH group were visible. These H-bond interactions were replaced with a double interaction by -SO_2- with Arg79 in case of compound **3**.-F group has participated in two hydrophilic halogen bond interactions with Glu53 and Gly80, and this was absent for the case of **3**. The latter was also stabilized with some hydrophobic interactions via indole and benzimidazole rings, in addition to similar ones to cyclopropyl in **CIP**, through cyclohexane (**Figure 3**). These profiles with both DNA-gyrase B subunit and Topo-IV ParE subunit provide us with some knowledge about the action mechanism of compound **3** as a dual inhibitor of these enzymes.

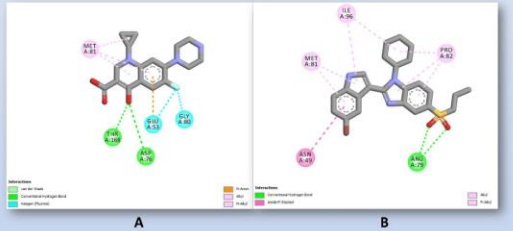

A B

Figure 3. Interacting residues of Topo-IV ParE with **CIP** (**A**) and compound **3** (**B**)

4. DISCUSSION

In this study, several indole-benzimidazole derivatives (**1-11**) with propylsulfonyl attachments were synthesized, structurally elucidated, microbiologically tested. For their potential utilization against nosochomial infections, two fundamental cell survival proteins of *S.aureus* were investigated in docking analysis. In the end, we have discussed biological activity results and potential dual inhibitor properties of our derivatives.

Using this standard in docking with DNA-gyrase and Topo-IV, higher activity of this derivative was spotlighted. As a result, this compound was able to bind to the active region of these enzymes with higher affinity (-8.1 kcal/mol for DNA-gyrase B subunit and -8.4 kcal/mol for Topo-IV) than that of Ciprofloxacin (-7.9 kcal/mol for DNA-gyrase B subunit and -7.3 kcal/mol for Topo-IV). Interaction-wise, the results were more promising for the modulation of DNA-gyrase B subunit since it has resembled the pattern. For DNA gyrase B subunit, indole hydrogen became rather important for the polar interactions. Indole and benzimidazole rings joined several stacking actions with hydrophobic residues of both enzymes. Substitution of the cyclopropyl group with cyclohexyl was proven to be useful for the modulation. According to this data, molecular necessities for the dual inhibition were understood. Consequently, compound **3** was found to be a candidate against nosochomial infection strain of *S.aureus* and was highlighted as a dual inhibitor of DNA-gyrase and Topoisomerase-IV.

REFERENCES

1. Levine C, Hiasa H, Marians KJ (1998). *Biochimica et Biophysica Acta - Gene Structure and Expression, 1400*(1-3), 29-43.
2. Hooper DC (1999). *Drugs*. 58 Suppl, 2:6–10.
3. Gibson EG, Bax B, Chan PF, Osheroı N (2019). *ACS Infect Dis*, 5, 570–581.
4. El AR, Aboul-Enein HY (2013). *Mini Rev Med Chem*, 13(3), 399-407
5. Charifson PS, Grillot A-L, Grossman TH, Parsons JD, Badia M, Bellon S, Deininger DD, Drumm JE, Gross CH, LeTiran A, Liao Y, Mani N, Nicolau DP, Perola E, Ronkin S, Shannon D, Swenson LL, Tang Q, Tessier PR, Tian S-K, Trudeau M, Wang T, Wei Y, Zhang H, Stamos D (2008). *Journal of Medicinal Chemistry, 51* (17), 5243-5263.
6. Bansal S, Sinha D, Singh M, Cheng B, Tse-Dinh YC, Tandon V (2012). *The Journal of Antimicrobial Chemotherapy*, *67*(12), 2882–2891.
7. Gullapelli K, Brahmeshwari G, Ravichander M, Kusuma U (2017). *Egyptian Journal of Basic and Applied Sciences*, 4(4), 303-309.
8. Ates-Alagoz Z, Buyukbingol Z, Buyukbingol E (2005). *Die Pharmazie*, 60, 643-647.
9. ISO 20776-1 (2006). Clinical laboratory testing and in vitro diagnostic test systems - Susceptibility testing of infectious agents and evaluation of performance of antimicrobial susceptibility test devices - Part 1: Reference method for testing the in vitro activity of antimicrobial agents against rapidly growing aerobic bacteria involved in infectious diseases.
10. Berman HM, Westbrook J, Feng Z, Gilliland G, Bhat TN, Weissig H, Shindyalov IN, Bourne PE (2000). *Nucleic Acids Research*, 28, 235-242.
11. Morris GM, Huey R, Lindstrom W, Sanner MF, Belew RK, Goodsell DS, Olson AJ (2009). *J Computational Chemistry*, 16, 2785-2791.
12. Hanwell MD, Curtis DE, Lonie DC, Vandermeersch T, Zurek E, Hutchison GR, *Journal of Cheminformatics*, 2012, 4, 17.
13. Trott O, Olson AJ (2010). *J Comp. Chem*, **31**, 455-461.
14. Dassault Systèmes BIOVIA, Discovery Studio Visualizer v17.2.0.16349, San Diego: Dassault Systèmes, 2017.
15. Sherer BA, Hull K, Green O, Basarab G, Hauck S, Hill P, Loch JT, Mullen G, Bist S, Bryant J, Boriack-Sjodin A, Read J, DeGrace N, Uria-Nickelsen M, Illingworth RN, Eakin, AE (2011). *Bioorganic & Medicinal Chemistry Letters*, 21(24).
16. Lu J, Patel S, Sharma N, Soisson SM, Kishi R, Takei M, Fukuda Y, Lumb KJ, Singh SB (2014). *ACS Chem Biol*, 9(9):2023-31.

PREPARATION OF SOME PURINE DERIVATIVES: USE OF THE 2D NMR $^{1}H,^{15}N$ & $^{1}H,^{13}C$ HMBC TECHNIQUES AND X-RAY CRYSTALLOGRAPHY IN ASSIGNING REGIOCHEMISTRY

[1]Doganc, F., [2]Sahin, E., [1]Goker, H.

[1]Ankara University, Department of Pharmaceutical Chemistry, Ankara, Turkey, doganc@ankara.edu.tr, goker@ankara.edu.tr

[2]Atatürk University, Department of Chemistry, Erzurum, Turkey, ertan@atauni.edu.tr

INTRODUCTION

Purines are basic component of nucleic acids and their many derivatives are used commercially as antiviral and antitumor drugs. Various tautomers of purine bases usually coexist due to the presence of several nitrogen atoms in the molecule. The preferred tautomers of purine derivatives are mainly *N*^{7}-H and *N*^{9}-H species, probably due to their lower energy. Existence of this tautomerism, in this bicyclic heterocycle has been shown with spectral data, mainly nuclear magnetic resonance (NMR) spectroscopy. This migration is disappeared when the imidazole hydrogen is replaced by alkyl groups. In our previous studies we reported the synthesis of some regioisomers of imidazole-containing heterocycles and their structural assignments were achieved by selective synthesis and/or 2D-NMR techniques (1-3). As a further contribution to this field, now we report the reaction of 2-(4-fluorophenyl) imidazopyrimidine with 4-chlorobenzyl bromide and the structural elucidation of regioisomeric products. Their structural assignments were made with the use of two-dimensional ^{1}H-^{1}H NOE (Nuclear Overhauser Effect Spectroscopy, NOESY) and ^{1}H-^{15}N HMBC (Heteronuclear Multiple Bond Correlation) spectra. Further confirmation of **1c** were obtained from X-ray crystallography.

MATERIAL AND METHODS

Synthesis of sodium metabisulfite adduct of 4-fluoro benzaldehyde

4-Fluorobenzaldehyde was dissolved in EtOH and sodium metabisulfite (in water) was added in portions. The reaction mixture was stirred vigorously and more EtOH was added. The mixture was kept in a refrigerator for a while. The white precipitate, the obtained salts were gained by filtration, dried and used for the further steps without purification and characterization.

8-(4-Fluorophenyl)-9*H*-purine 1

The mixture of sodium metabisulfite adduct of 4-fluorobenzaldehyde and 4,5-diamino-pyrimidine, in DMF were heated at 120°C, for 3-4 h. The reaction mixture was cooled, poured into water. The resulting precipitate was collected by filtration and boiled in EtOH filtered and dried.

9-(4-Chlorobenzyl)-8-(4-fluorophenyl)-9*H*-purine (1a), 3-(4-Chlorobenzyl)-8-(4-fluorophenyl)-3*H*-purine (1b) and 1-(4-Chlorobenzyl)-8-(4-fluorophenyl)-1*H*-purine (1c)

K_2CO_3 was added to a suspension of 8-(4-Fluorophenyl)-9*H*-purine **(1)** in DMF and stirred. One hour later, 4-chlorobenzyl bromide was added. After overnight stirring at room temperature, water was added and precipitate was filtered. Crude solid powder was purified by column chromatography.

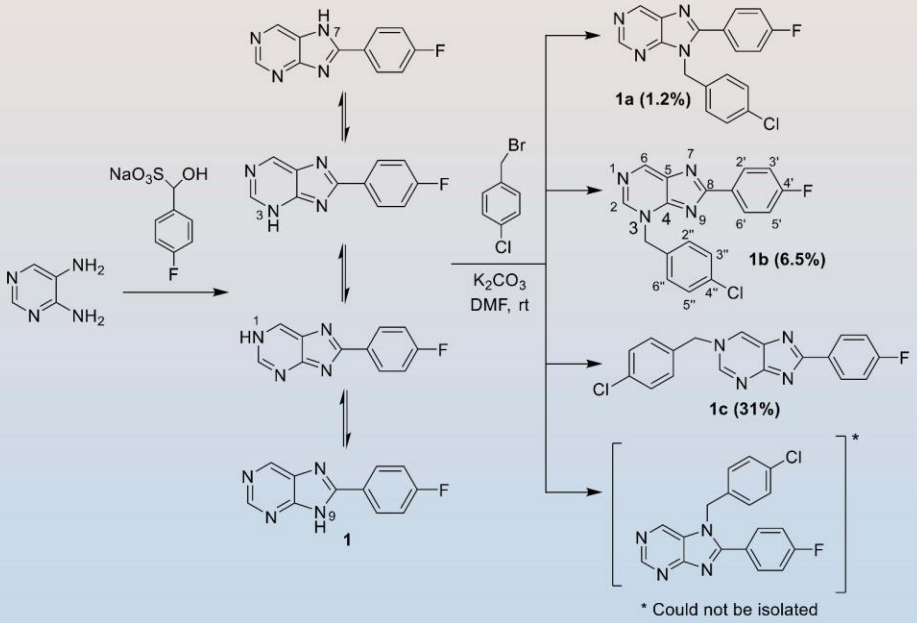

Scheme 1. Synthesis of 8-(4-fluorophenyl)purine analogues.

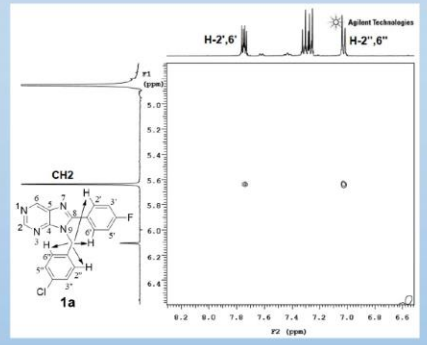

Fig. 1 NOESY spectra of compounds **1a** (CD_3OD).

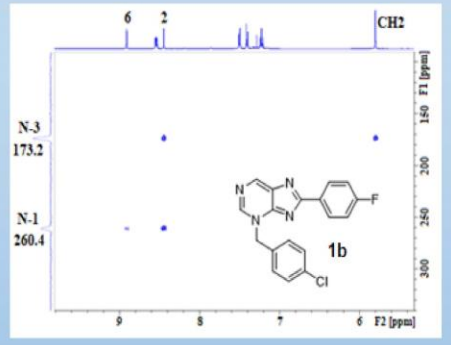

Fig. 2 ^{1}H-^{15}N HMBC spectrum of compounds **1b** ($CDCl_3$).

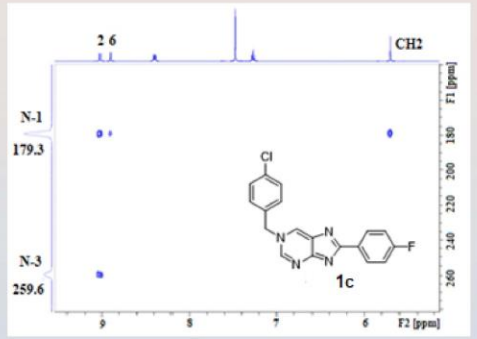

Fig. 3 ^{1}H-^{15}N HMBC spectrum of compounds **1c** (CD_3OD).

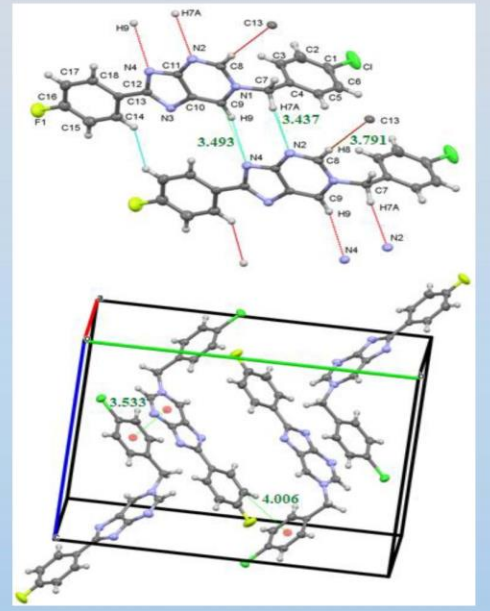

Fig. 4 Up) Molecular structure of **1c** with the short contact geometry (less than the sum of vdW radius). **Down)** C-H···π and π-π stacking interactions of the molecule **1c** with the unit cell viewed down along the a-axis.

RESULTS AND DISCUSSION

Targeted compounds were prepared using the methods outlined in Scheme 1. We achieved three regioisomeric products (**1a-c**) and results were confirmed by NOESY and HMBC correlations (Figs. 1, 2 and 3). The results obtained from the HMBC spectra of **1(b-c)** provided all expected correlations. ^{1}H-^{15}N HMBC correlations also confirmed the proposed structures of the regioisomers. Further confirmation of the structure of **1c** was obtained from X-ray crystallography (Fig. 4). Its suitable crystal was grown from $CHCl_3$ solution. Structure of **1c** was solved in the monoclinic space group $P2_1/c$. Purine ring is almost in the same plane as the 4-fluorophenyl group. The dihedral angle between the chlorophenyl and purine mean planes is 85.2°. C=N double bonds in the ring are as follows ; N4=C11 1.328(3) Å, N3=C12 1.335(3) Å and N2=C8 1.302 Å. Meanwhile, intermolecular C7-H···N1 [*D*···*A* = 3.437(3) Å], C9-H···N4 [*D*···*A* = 3.493(3) Å] and C-H···π (4.0 Å) interactions have a contribution in the formation of a stable structure. The π-π stacking distances are in the range of 3.53-5.97 Å.

CONCLUSION

Imidazole *N*-alkylated regioisomers were obtained in presence of anhydrous K_2CO_3 in DMF. In our experiments, imidazole *N*-alkylated regioisomers were obtained firstly from the column chromatography. NOESY experiment is the primary method for structural elucidation of these types of regioisomers. The cross peaks of *N*-CH_2 (at around 5-6 δ ppm) and aromatic protons confirm their spatial proximity as an evidence for which nitrogen atom is substituted. ^{1}H-^{13}C and ^{1}H-^{15}N HMBC techniques can be an effective alternative method for assignment of regioisomers. The complete structure elucidation of all synthesized compounds was performed using 1D and 2D NMR experiments including COSY, NOESY, gHSQC, gHMBC and XRD data.

ACKNOWLEDGEMENT

Central Laboratory of Faculty of Pharmacy of Ankara University provided support for the acquisition of the NMR and mass spectrometer used in this work.

References

1. Doganc F, Alp M et al. (2016). Magnetic Resonance in Chemistry 54:851-857.
2. Göker H, Özden S (2019). Journal of Molecular Structure 1197:183-195.
3. Karaaslan C, Doganc F et al. (2020). Journal of Molecular Structure 1205:1-13.

DESIGN, SYNTHESIS AND ANTIMICROBIAL EVALUATION OF NOVEL ISOQUINOLIN-UREA HYBRIDE MOLECULES

[1]Han Mİ*., [2]Dengiz Ç., [3]Doğan ŞD., [4]Gündüz MG., [5]Özkul C.

[1] Erciyes University, Department of Pharmaceutical Chemistry, Kayseri, Turkey, hanihsan@gmail.com

[2] Middle East Technical University, Department of Chemistry, Ankara, Turkey, dengizc@metu.edu.tr

[3] Erciyes University, Department of Basic Sciences, Kayseri, Turkey, dogandilem@erciyes.edu.tr

[4] Hacettepe University, Department of Pharmaceutical Chemistry, Ankara, Turkey, miyaseg@hacettepe.edu.tr

[5] Hacettepe University, Department of Pharmaceutical Microbiology, Ankara, Turkey, cerenozkul@hacettepe.edu.tr

*Presenter e-mail hanihsan@gmail.com

1. INTRODUCTION

As microorganisms have developed resistance to antimicrobial drugs in recent years, it has become very important to introduce new molecules to medical use. Lack of novel drug molecules and synthesis of molecules without important effects canalized researchers to develop new molecules in this area. It has been reported in studies that molecules with urea structure have antimicrobial activities [1].

2. METHODS

1H-2-benzopyran-1,3(4H)-dione (BPD) was used as the starting compound to synthesis new urea molecules. The reaction of BPD with hydrazine-hydrate in ethanolic medium resulted in 2-aminoisoquinoline-1,3(2H,4H)-dione (AQD) [2]. AQD was refluxed with substituted various isocyanates in toluene at 80 °C (QU1-22) [3] (**Figure 1, Table 1**). The synthesized molecules evaluated antimicrobial activity against S. aureus, MRSA, E. faecalis and E. coli.

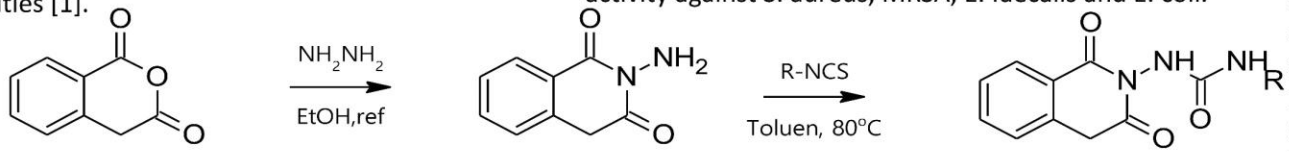

Figure1. Synthesis route of new ısoquinolin molecules

3. RESULTS

The structures of the compounds QU1-22 were determined by spectroscopic and spectrometric techniques such as ^{1}H-NMR, ^{13}C-NMR and HR-MS. Two of the targeted compounds showed antimicrobial activity with good results (**Table 2**).

4. DISCUSSION

New isoquinoline-urea derivatives (QU1-22) were synthesized, characterized and their antimicrobial activity was evaluated.

1H-2-benzopyran-1,3(4H)-dione (BPD) was used as the starting compound to synthesis 2-aminoisoquinoline-1,3(2H,4H)-dione (AQD) and new urea molecules (QU1-22). They were registered to interested literatures (2,3). ^{1}H-NMR spectral data of compounds QU1-22 revealed supporting to evidence to identify their structures. The singlet signals belonging to –NH urea protons were detected at 10.07-8.03 and 8.09-9.26 ppm. ^{13}C-NMR spectral data of compounds QU1-22 the singlet signals belonging to C=O carbon signals were detected at 168.76-168.90, 163.74-163.97 and 155.87-152.88 ppm. Among the synthesized molecules, two of them were found to have 8 MIC values of antimicrobial activity.

COMPOUND	R-	COMPOUND	R-
QU1	-C_6H_5	QU12	-C_6H_5-CN(4)
QU2	-C_6H_5-t-buthyl	QU13	adamanthyl
QU3	-t-buthyl	QU14	-C_6H_5-CN(4)
QU4	-C_6H_5-CH_3(2)	QU15	-C_6H_5-CH_3(2,6)
QU5	allyl	QU16	-C_6H_5-Cl(4),CF_3(3)
QU6	-C_6H_5-CF_3(4)	QU17	-C_6H_5-CH_3(3)
QU7	-C_6H_5-F(3)	QU18	-C_6H_5-CF_3(3,5)
QU8	-C_6H_5-Cl(3)-F(4)	QU19	-C_6H_5-OCH_3(2,4)
QU9	-C_6H_5-OCH_3(2)	QU20	-C_6H_5-NO_2(3)
QU10	-C_6H_5-CF_3(3)	QU21	naphtyl
QU11	-C_6H_5-CF_3(2)	QU22	-C_6H_{11}

Table 1. Structures of compounds QU1-22

COMPOUNDS	S. aureus ATCC 29213	MRSA ATCC 43300	E. faecalis ATCC 29212	E. coli ATCC 25922
QU1	128	128	128	128
QU2	128	128	256	512
QU3	512	256	256	512
QU4	256	256	256	256
QU5	512	256	256	512
QU6	256	256	256	1024
QU7	256	256	256	256
QU8	512	256	256	512
QU9	256	256	256	256
QU10	256	512	512	512
QU11	256	128	256	512
QU12	256	128	128	256
QU13	256	128	128	256
QU14	512	256	256	512
QU15	256	256	256	512
QU16	**32**	**8**	**32**	**1024**
QU17	256	256	128	256
QU18	**64**	**8**	**64**	**256**
QU19	256	128	256	256
QU20	256	256	256	256
QU21	256	128	512	512
QU22	256	128	256	256
Piperacillin-tazobactam	0,125	NA	0,25	0,25
Gentamicin	0,5	32	8	0,5

Table 2. Antimicrobial activity results of compounds QU1-22

References

1.Gunduz MG, Uğur SB, Guney F, Ozkul C, Krishnad VS, Kaya S, Sriram D, Doğan ŞD (2020). Bioorganic Chemistry, 102: 104104.

2.Ozcan S, Dengiz Ç, Deliömeroglu MK, Sahin E, Balci M (2011). Tetrahedron Letters, 52: 1495–1497.

3.Doğan ŞD, Buran S, Gunduz MG, Ozkul C, Krishna VS, Sriram D (2019). Chem. Biodiversity, 16, e1900461.

Deep Eutectic Solvents as powerful catalysts and solvents for the synthesis of amides

[1]Procopio, D., [2]Nardi, M., [2]Oliverio, M., [2]Procopio, A. and [1]Di Gioia, M.L.

[1] University of Calabria, Department of Pharmacy, Health and Nutritional Sciences, Arcavacata of Rende (CS), Italy, [2]University Magna Graecia, Department of Health Sciences, Catanzaro, Italy. E-mail: debora.procopio@unical.it

Introduction

The amide bond represents the main structural motif in small molecule API drugs and therapeutic peptides. The growing need for large amounts of biologically active amides and peptides for the pharmaceutical market has strongly raised the issue of the environmental sustainability of their synthesis. Current methods suffer from low efficiency and sustainability and generate large amounts of waste products, where solvents are the major source.

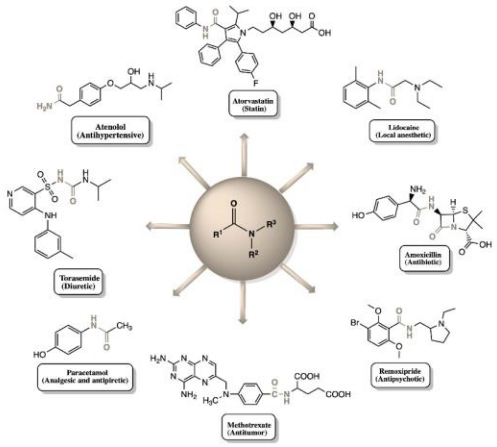

Aim of the work

The work aims to develop an eco-friendly method for the synthesis of amides through the use of DES as a reaction medium. More specifically, the roles that DES can assume in the context of this transformation were investigated, i.e. as a solvent and catalytic medium or as a solvent and reagent.

Methods

- DES formation

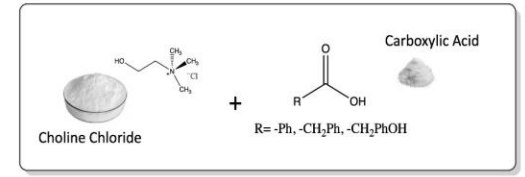

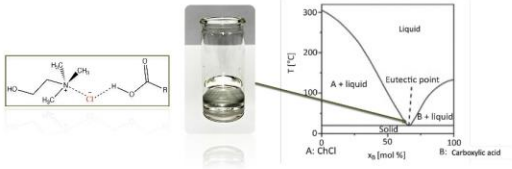

Deep eutectic solvents (DESs) have been prepared by mixing choline chloride, used as Hydrogen Bond Acceptor (HBA), and different carboxylic acids used as Hydrogen Bond Donor (HBD).

- Coupling reaction

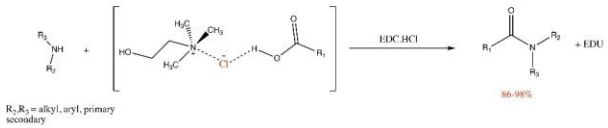

Reactions were performed by adding the EDC (1mmol) to the DES and, at the same time, the amine (1mmol). The resulting mixture is kept under magnetic stirring at a temperature of 40 ° C, in a water bath. Reactions are monitored by TLC until the reaction is complete. At the end of the reaction the addition of water in the reaction mixture enables amide precipitation, while EDU and ChCl remain in water.

- Amides Characterization

All obtained amides were characterised by GC-MS and NMR analysis, resulting pure without the need of further chromatographic purification.

Results and Discussion

Deep eutectic solvents (DES) represent a promising eco-friendly alternative to conventional solvents. They can be used not only as reaction media, but also as active catalytic species and, in some cases, as reagents. Herein, we evaluated for the first time the dual role of DESs as reaction media and reagent in the 1-ethyl-3-(3-dimethylaminopropyl)carbodiimide (EDC) mediated synthesis of amides. All the reactions tested proceed at low temperatures and in a short time without the need for a basic catalyst. The reaction conditions demonstrate compatibility with a wide range of carboxylic acids and amines, affording the desired amides in excellent yields (86-98%).

Conclusions

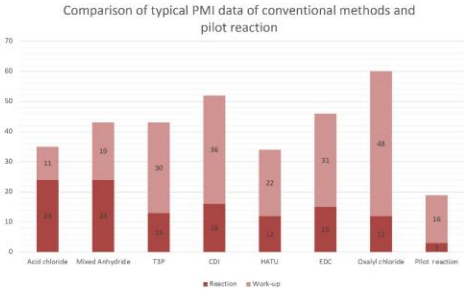

A highly efficient, mild, catalytic protocol has been developed for the synthesis of amides using a reactive DES. The advantages of this procedure include environmental compatibility, versatility, and easy workup.

References

- Bryan, M.C. *et al*. Key Green Chemistry research areas from a pharmaceutical manufacturers' perspective revisited. Green Chem., 2018, 20, 5082–5103;
- Lau, J. L. *et al*. Therapeutic peptides: Historical perspective, current development trends, and future directions. Bioorganic & Medicinal Chemistry, 2018, 26, 2700–2707
- Prat, *et al*. CHEM21 selection guide of classical- and less classical-solvents. Green Chem., 2016, 18, 288–296
- Emami *et al*. Deep Eutectic Solvents for Pharmaceutical Formulation and Drug Delivery Applications. Pharmaceutical Development and Technology, 2020;

SYNTHESIS OF PLATINUM(II) COMPLEXES WITH 2-SUBSTITUTED BENZIMIDAZOLE LIGANDS

[1]Özçelik AB.,[1]Akdağ M., [2]Utku S.
[1]Gazi University,Department of Pharmaceutical Chemistry, Faculty of Pharmacy, Ankara, Turkey, azime@gazi.edu.tr, mevakd@hotmail.com
[2] Mersin University, Department of Pharmaceutical Chemistry,Faculty of Pharmacy, Mersin,Turkey, utkusemra@hotmail.com

INTRODUCTION

The discovery of cisplatin, also known as cis-[Pt(NH3)2Cl2], was a milestone in the development of platinum(II) and other metal-containing complexes as potential anticancer drugs. Among these complexes, only carboplatin and oxaliplatin have received worldwide approval so far, nedaplatin, loboplatin and heptaplatin have gained regionally limited approval (1).

It is well established that cisplatin binds to DNA via covalent bonding, forming mostly 1,2-intrastrand cross-links, which deforms the DNA structure, preventing DNA replication and transcription, and activates the apoptotic pathway, resulting in cell death (2). The replacement of amine groups can result in different structural and formational alterations in target DNA, which may affect the character of biological effects of the analogues(3).

One noteworthy approach in the design of new platinum anticancer drugs is to use physiologically active compounds as ligands. The benzimidazole ring is a physiologically active ligand found in the structure of vitamin B12 and its derivatives, purin bases, and several metalloproteins. It also serves as a good ligand in various transition metal complexes (4).

In accordance with our previous studies, considering that variations in the chemical structure of the amine groups of cisplatin might have a significant effect on the cytotoxic activity and toxicity of platinum complexes and with the aim of determining the role of the benzimidazole ligands of platinum(II) complexes on cytotoxic properties, we synthesized some platinum(II) complexes with 2-substitutedbenzimidazole ligands.

In this study, platinum(II) complexes having 2-(2 or 4-trifloromethyl)phenylsubstituted benzimidazoles carrier ligands were designed and synthesized by us. Chemical structures of the complexes were elucidated by their IR, ^{1}H-NMR, Mass spectroscopic methods.

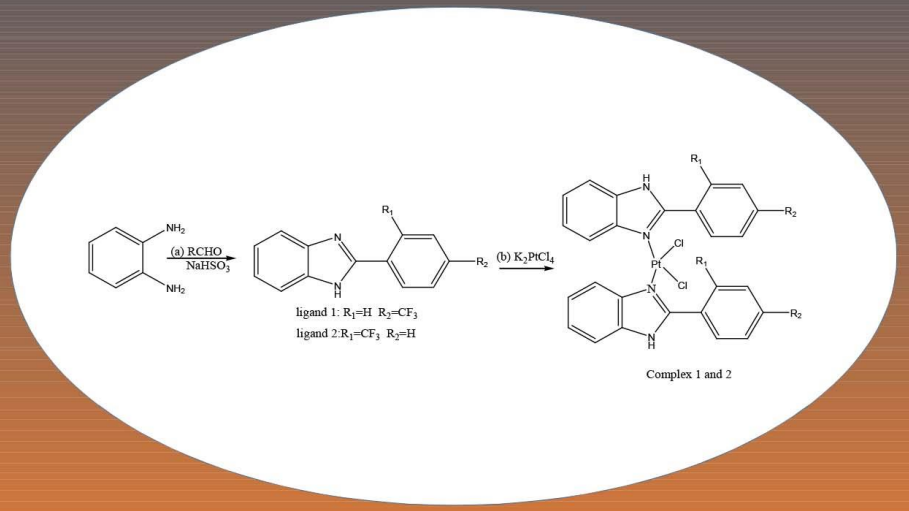

CONCLUSION

As a result, based on the spectral data obtained in this study, synthesized complexes have been shown to have a desired purity and molecular structure.

ACKNOWLEDGEMENT

.
Mevlüt Akdağ is a PhD fellow of YÖK 100/2000 scholarship program.

REFERENCES

1. Deo KM., Ang, DL, et al., (2018). Coordination Chemistry Reviews, 375:148-163.
2. Yu C, Wang Z, et al., (2020). Journal of Medicinal Chemistry, 63 (22):13397-13412.
3. Ghosh S (2019). Bioorganic chemistry, 88:102925.
4. Curini R, Materazzi S, etal.,(1990). Thermochimica Acta , 161(2):201-374.
5. Lippert B. (1989), Platinum Nucleobase Chemistry. Prog. Inorg. Chem. **37**, 1-97.
6. Callaghan, V.; Goodgame, D. M. L.; Tooze, R. P.: Inorg. Chim. Acta 78, 51 (1983)

MATERIALS AND METHODS

2 mmol of corresponding ligands and 1 mmol of K_2PtCl_4 were dissolved in isopropylalcohol-water. The reaction mixture protected from light was heated at 60 ^{0}C for 7 days. The resulting precipitate was filtered off, washed several times with small portions of water, ethanol, and diethylether and dried in vacuo.

RESULTS

In the present paper, two platinum(II) complexes, *cis*-[PtL_2Cl_2] (L=2-substitutedbenzimidazole as “non-leaving groups), were designed and synthesized. The chemical structures of Pt(II) complexes were elucidated by using IR, ^{1}H- NMR and LC/MS spectroscopic methods. In the IR spectra of synthesized complexes, prominent changes were observed. The ^{1}H-NMR spectra of these complexes were consistent with their corresponding protons as chemical shift values and the number of hydrogens. Both the retention times and the MS spectra of the peaks in samples are evidence of the purity and the expected structures of the synthesized compounds. The ^{1}H-NMR spectra of the complexes revealed considerable differences from those of the free ligands. The large downfield shifts in the imidazole N1-H signal of the complexes compared to their ligands are the result of an increase in the N1-H acidic character after platinum binding (5). The changes in the chemical shift observed upon coordination ($\Delta\delta = \delta$ complex – δ free ligand) are mostly positive, indicating a decrease in electronic density on the 2-substituted benzimidazole ligands upon coordination of the platinum. The NH signal is observed at approximately 12 ppm in L_1 and L_2, and it has been determined that it shifts downfield at 13.2 and 13.4 ppm in complexes 1 and 2, respectively. In the far IR region of the complexes’ spectra a new band appeared assigned to Pt—Cl stretching bands, centered at 320 cm^{-1} and characteristic for cis configurated dichloro-Pt(II) complexes (6).

SYNTHESIS AND ANTICANCER ACTIVITY OF ETODOLAC HYDRAZONES

[1]Hande Cevher Koç, [2]İrem Atlıhan, [3]Pınar Mega-Tiber, [3]Oya Orun, [4]Ş. Güniz Küçükgüzel

[1] Marmara University, Institute of Health Sciences, Department of Pharmaceutical Chemistry, Istanbul, Turkey [2] Marmara University, Institute of Health Sciences, Department of Biophysics, Istanbul, Turkey [3] Marmara University, Faculty of Medicine, Department of Biophysics, Istanbul, Turkey [4] Fenerbahçe University, Vocational School of Health Services, Istanbul, Turkey

e-mail: handec.koc@gmail.com

INTRODUCTION

Deaths from cancer cases tend to increase gradually. In order to break this negative chain, the focus has been on various derivatives that can be strong candidates as cancer drugs. Hydrazide-hydrazone is one of the most prominent structures among these derivatives. The anticancer activity of hydrazide-hydrazone compounds results from its active pharmacophore group (-CO-NH-N=CH-) (1). According to results of many studies, the antitumor effects of hydrazide-hydrazones have been proved (2-5). Therefore, it is aimed to synthesize new hydrazide-hydrazone compounds choosing etodolac as a starting compound and to determine their possible anticancer activity against PC-3, DU-145, LNCaP prostate cancer cells.

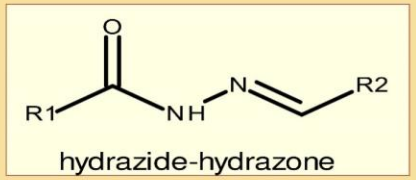

hydrazide-hydrazone

METHODS

Etodolac methyl ester **[1]** was obtained by the reaction of etodolac and methanol in the presence of concentrated sulfuric acid. Etodolac hydrazide **[2]** was synthesized by heating compound **1** with hydrazine hydrate in methanol. After compound **2** and substituted benzaldehydes were refluxed in ethanol medium, etodolac hydrazide-hydrazones **[3a-l]** were obtained.

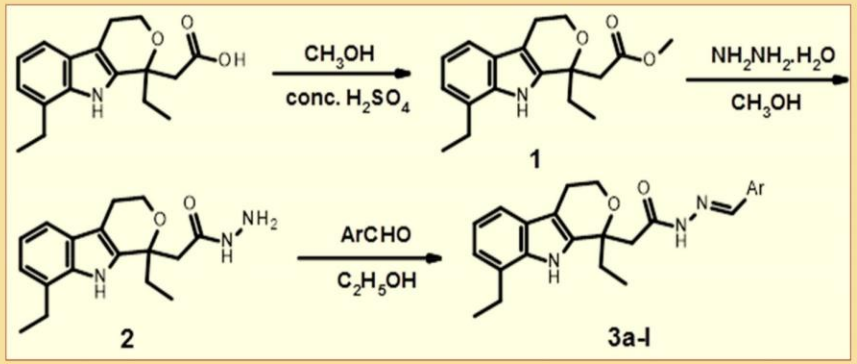

Ar					
3a	2,4-Dichlorophenyl	**3e**	2-Chloro-3-methoxyphenyl	**3i**	2,5-Dimethoxyphenyl
3b	2,6-Dichlorophenyl	**3f**	4-Methoxy-3-nitrophenyl	**3j**	2,6-Dimethoxyphenyl
3c	3,4-Dichlorophenyl	**3g**	5-Bromo-2-methoxyphenyl	**3k**	3,4-Dimethoxyphenyl
3d	4-Bromophenyl	**3h**	3-Hydroxy-4-methoxyphenyl	**3l**	2,4,6-Trimethylphenyl

The cytotoxic effects of **3a-l** → WST-8 test
The apoptotic effect of **3b** → JC-1 mitochondrial membrane potential test.

RESULTS

IC_{50} values of compounds **3a-l** (μM)			
comp.	**PC-3**	**DU-145**	**LNCaP**
3a	28.68	30.38	20.48
3b	10.36	5.24	15.53
3c	22.31	33.65	25.46
3d	20.79	11.39	19.81
3e	17.22	21.60	37.91
3f	21.27	30.44	28.94
3g	57.29	45.75	38.70
3h	54.82	29.45	67.16
3i	76.92	40.35	>100
3j	45.20	43.51	45.89
3k	25.62	16.51	29.93
3l	10.20	15.33	34.11

Compound **3b** was found to display higher cytotoxicity against three prostate cancer cells and cause depolarization on mitochondrial membrane potential.

DISCUSSION

The novel etodolac hydrazones were synthesized, their structures were characterized by spectroscopic methods, besides elementel analysis and their anticancer effects on prostate cancer cells were evaluated. According to these results, compound **3b** was hydrazide-hydrazone found to be an effective derivative.

REFERENCES

1.Rollas S, Kucukguzel SG (2007). Molecules, 12:1910-1939. **2**.Cıkla P et al. (2013). Arch Pharm (Weinheim), 346:367-379. **3**.Aydın S et al. (2013).Marmara Pharm J, 17:181-189. **4**.Kucukguzel SG et al. (2015). Arch Pharm (Weinheim), 348:730-742. **5**.Senkardes S et al. (2016) Eur J Med Chem, 108:301-308.

SYNTHESIS AND MOLECULAR MODELING STUDIES OF SOME NOVEL BENZOTHIAZOLE DERIVATIVES AS ANTI-CANCER AGENTS

[1]Yenice Cakmak G., [2]Yilmaz S., [3]Yildiz I.

[1] Trakya University, Department of Pharmaceutical Chemistry, Edirne, Turkey, gozdeyenice@trakya.edu.tr

[2] Trakya University, Department of Pharmaceutical Chemistry, Edirne, Turkey, serapyilmaz@trakya.edu.tr

[3] Ankara University, , Department of Pharmaceutical Chemistry, Ankara, Turkey, iyildiz@pharmacy.ankara.edu.tr

JUNE 22-25, 2021 ANKARA, TURKEY

ISOPS 13th International Symposium on Pharmaceutical Sciences

INTRODUCTION

Cancer is a major public health problem in many areas of the World. It is a complex disease characterized by dysregulation of cell proliferation and cell death, and ultimately transforms into a population of cells that can invade the tissues and metastasize to distant areas, leading to severe morbidity [1]. It can occur in the various organs and systems of the body, and result in death of the host if could not be treated. In the clinic, cancer appears to be different diseases with different phenotypic features. However, all cancers have many common characteristics at the molecular level [2]

Topoisomerase enzymes have shown unique roles in replication and transcription [3]. Inhibitors targeting human topoisomerase I and topoisomerase II alpha have provided a useful chemotherapy option for the treatment of many patients suffering from a variety of cancers [4]. Heterocyclic compounds are commonly found in major structures and have important roles in medial chemistry due to their pharmacological activities [5]. In our study, some benzathiazole derivatives were designed to develop new anticancer drugs, in silico activities against Topoisomerase II enzyme were observed with molecular modeling studies; and cytotoxic activities was evaluated by comparison with reference compound etoposide using MTT method on cell lines.

MATERİALS AND METHODS

Method A: Synthesis of 2-(4-Aminobenzyl)benzothiazole compound.

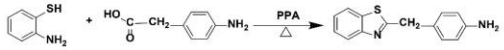

Method B: Synthesis of N-(4-(benzothiazol-2-ylmethyl)phenyl)amide derivative compounds

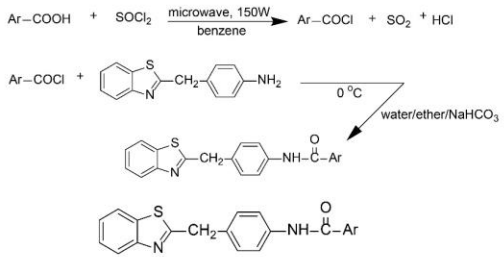

Ar-					
1		4	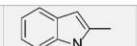	9	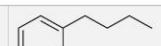
2		6	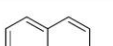	10	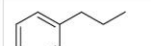
3		8		11	

Figure 1. Synthesized Compounds (1-11)

Molecular Docking Processes

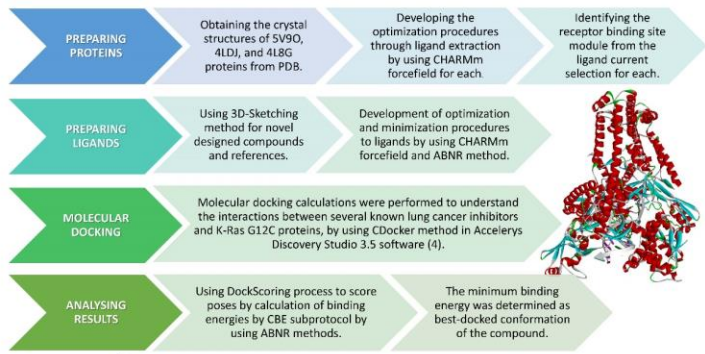

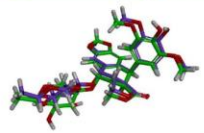

Figure 2. The X-Ray crystallography structure of etoposide and docked etoposide with 0,68 Å RMSD value means the the docked position of etoposide overlaps well with the crystal structure position.

RESULTS & DISCUSSION

Synthesis of N- (4- (benzothiazol-2-ylmethyl) phenyl) amide derivatives, analysis of their structures; investigation of their anticancer activities were performed. The biological action mechanism elucidation studies were carried out using molecular docking techniques on Topoisomerase-II.

Compound no / Cell line	1	2	3	4	6	8	9	10	11	etoposide
A549	95,05	93,40	82,39	67,61	95,52	97,88	130,27	104,72	102,6901	95,01
MCF-7	99,21	100,58	79,84	75,81	82,00	98,42	114,76	110,66	102,486	100,40
PC-3	84,68	89,71	77,38	71,93	83,45	104,08	110,19	111,52	90,39301	*
HEP-3B	184,70	167,70	162,69	166,15	155,45	126,54	153,28	134,73	93,11562	*
HELA	110,76	145,53	100,06	98,47	119,48	133,98	145,75	101,13	100,6693	99,73
HT-29	89,23	89,94	83,60	73,90	93,09	97,05	81,62	83,60	89,46299	93,97
K562	106,57	92,13	70,19	53,52	64,86	76,62	96,44	73,33	104,17	97,97
Raji	87,04	100,20	82,54	77,59	68,11	66,92	84,92	74,62	107,83	104,73
NIH3T3	91,86	100,46	80,27	88,87	95,44	103,78	105,14	102,41	98,83833	*

Table 1. IC50 values measured in various cells after MTT analysis of synthesized compounds (c: compound, h: cell line)

Compound	Binding Energies
1	-48,5679
2	-47,6865
3	-95,1796
4	-92,2613
6	-84,3315
8	-52,4095
9	-78,1374
10	-54,5615
11	-83,2909

Table 2. Binding energies of synthesized compounds (1-11) obtained after docking on 3QX3 protein by molecular modeling

Compound	Binding Energies	Interactions
3	-95,1796	DA12[b], DG13[b], DC8[b], DT9[b,d], ARG503[a,f], DC11[c],DG10[c]
4	-92,2613	ARG503[a,f], DG13[b], DA12[b], DC8[b], DT9[b,d,g], GLN778[a], MET782[a]

Table 3. Interaction sites of Compounds 3 and 4 on the 3QX3 protein
a: Conventional H bond, b: π-π Stacked, c: Carbon Hydrogen bond, d: π-π T shaped, e: π-alkyl, alkyl, f: π-cation, g: π-sulfur, h: π -donor H bond, i: Water-H bond, j: π-anion

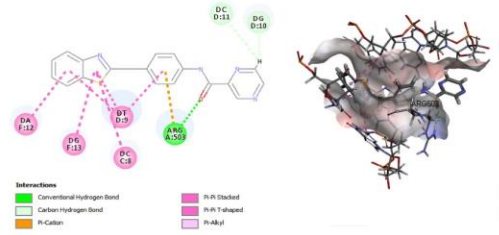

Figure 3. 2D and 3D view of the interaction of Compound 3 with the active site of the 3QX3 protein

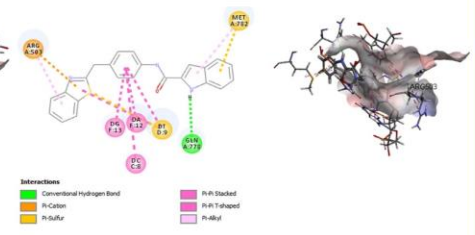

Figure 4. 2D and 3D view of the interaction of Compound 4 with the active site of the 3QX3 protein

Physicochemical and Pharmacokinetic Parameters

It is necessary to keep the various physicochemical properties at the optimum level in order to have high biological activities and low toxic effects of the compounds developed as drugs, and to show maximum oral bioavailability. For this reason, the synthesized compounds were evaluated by filters developed by some researchers according to druglikeness.

Compound	Log P	Molecular Weight (MW)	Hydrogen Bond Acceptor (HBA)	Hydrogen Bond Donor (HBD)	Rotatable Bonds	Aromatic Ring Number	Polar Surface Area (PSA)
1	4,61	350,46	2	1	4	4	41,37
2	4,05	334,39	2	1	4	4	53,93
3	2,79	346,41	4	1	4	4	63,89
4	5,24	383,47	2	2	4	5	56,43
6	5,57	394,49	2	1	4	5	41,37
8	5,25	384,45	2	1	4	5	53,93
9	5,61	386,51	2	1	7	4	41,37
10	5,15	372,48	2	1	6	4	41,37
11	5,59	416,54	3	1	8	4	50,30

Table 3. Physicochemical Parameters of Synthesized Compounds

CONCLUSIONS

The structures of 9 original N-(4-(benzothiazol-2-ylmethyl)phenyl)amide derivative compounds synthesized in the study were elucidated using 1H-NMR, 13C-NMR and Mass Spectroscopy, and the structures of A549 (Human lung carcinoma), MCF-7 (Human breast cancer) were elucidated. adenocarcinoma), PC-3 (Human prostate cancer), HEP-3B (Human hepatocellular carcinoma), HeLa (human cervical cancer), HT-29 (human colorectal adenocarcinoma), K562 (Human bone marrow chronic myeloid leukemia), Raji (human Burkitt lymphoma), NIH3T3 (mouse embryo fibroblast) cell lines, the anticancer activities were calculated as IC50 values by applying the MTT test, and the mechanism of the biological effect was tried to be clarified by using molecular docking techniques on the Topoisomerase-II protein in line with the biological activity results.

According to the cytotoxic activity results; the activity of compounds 3 and 4 and 6 in the K562 cell line and the compound 4 in the A549 cell line were observed. In docking studies, compounds 3 and 4 show interactions with the Topo II (pdb: 3QX3) proteins at low energies, suggesting that compounds 3 and 4 can act via the Topo II enzyme pathway.

ACKNOWLEDGEMENTS

This study was not supported by any institution or organization.

REFERENCES

1. Ruddon RW. (2007) *Cancer biology*, Oxford University Press.
2. Chohan TA, Qian H, Pan Y, Chen JZ, Cyclin-dependent kinase-2 as a target for cancer therapy: progress in the development of CDK2 inhibitors as anti-cancer agents. Curr. Med. Chem., 2015; 22(2): p. 237-63.
3. Dehshahri A, Ashrafizadeh M, et.al. (2020). Topoisomerase inhibitors: Pharmacology and emerging nanoscale delivery systems. *Pharmacological research*, *151*, 104551.
4. Wang W, Tse-Dinh YC. (2019). Recent advances in use of topoisomerase inhibitors in combination cancer therapy. *Current topics in medicinal chemistry*, *19*(9), 730-740.
5. Ali, RN Siddiqui, Biological Aspects of Emerging Benzothiazoles: A Short Review. Vol. 2013.

JUNE 22-25, 2021
ANKARA, TURKEY
ISOPS 13th International Symposium on Pharmaceutical Sciences
Ankara University Faculty of Pharmacy

A MONTMORILLONITE CLAY AS AN EFFICIENT AND GREEN CATALYST FOR FUNCTIONAL POLYETHER SYNTHESIS

[1,2] Belbekiri Habiba, [2] Rachid Meghabar and [2] Mohamed Belbachir
[1] [2] Department of Material Sciences, Faculty of Exact Sciences, University of Tahri Mohamed , B.P. 417, Bechar, Algeria
Laboratoire de Chimie des Polymères, Département de Chimie,Université d'Oran 1, Ahmed Ben Bella, BP N° 1524 El M'Naouar, Oran, Algeria
belbekirih@yahoo.fr

Introduction

One of the major current challenges before chemists is to develop synthetic methods that are less polluting, i.e., to design clean or 'green' chemical transformations. Green chemistry simply, is the use of chemistry techniques and methodology that reduce or eliminate the use or generation of feedstock, products, by-products, solvents and reagents (1). that are hazardous to human health or the environment (Anastas,Williamson, 1996) . In efforts aimed at the development of new drug compounds, pharmaceutical companies and academic research labs also generate a significant amount of chemical waste that is hazardous to the environment. Since the Pollution Prevention Act of 1990 was passed, however, chemists have attempted to minimize waste by designing new, more environmentally friendly methods for synthesizing useful organic compounds (2).

The purpose of this study was to synthesize polyether by green catalysis, based on the ring opening polymerization of terahydrofurane with epichlorhydrin by an environment-friendly solid catalyst (Maghnite-H$^+$). "Maghnite" a montmorillonite sheet silicate clay, exchanged with protons to produce "Maghnite-H$^+$" is an efficient catalyst for cationic polymerization of many vinylic and heterocyclic monomers (Belbachir, M. *U.S. Patent.* 066969.0101 –2001). This solid catalyst can be easily separated from the polymer products and regenerated by heating to a temperature above 100 °C (3,4). The effects of the relative amounts of the Maghnite-H$^+$ on the outcome of the polymerization are also discussed. The synthesized polyether was characterized by infrared spectroscopy (IR), 1H-NMR spectroscopy.

Materials and methods

•The preparation of the ''Maghnite-H$^+$ ''(sheme 1) was carried out by using a method similar to that described by Belbachir et al (4).

•Epichlorhydrin (99%),Tetrahydrofurane (99%) and acetic anhydride were purchased from Prolabo in 99% purity.

•The ring opening bulk copolymerization of tetrahydrofurane with epichlorhydrine was carried out in sealed tubes at room temperature, using a Maghnite-H$^+$ as initiator (sheme 2). This solid catalyst can be easily separated from the polymer products and regenerated.

Step.1: (20 g) was crushed for 20 min using a prolabo ceramic balls grinder.

Step.2: It was then dried for 2h at 105°C. The Maghnite was placed in an erlenmeyer flask together with 500 ml of distilled water

Step.3 : The maghnite/water mixture was stirred using a magnetic stirrer and combined with 0.25 M H2SO4 solution, over 2 days, the mineral was then washed with distilled water and then dried at 105 °C.

Scheme1: Steps of the preparation of the Maghnite-H$^+$

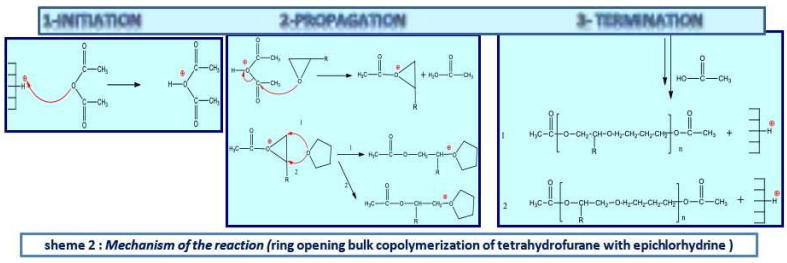

sheme 2 : *Mechanism of the reaction* (ring opening bulk copolymerization of tetrahydrofurane with epichlorhydrine)

Results and discussion

The results of bulk copolymerisation experiments of tetrahydrofurane with epichlorhydrine is provided as follows :

According to the work published by Hamilton and Semlyen (5),The copolymer (poly(THF-co-ECH)) reveals characteristic resonance lines for the methyl groups of the ECH (CH_2Cl) repeating units at δ = 3.65ppm, the central methylene groups of THF at δ = 1.62 ppm, The complex signal that resonates between 3.40 and 3.7 ppm corresponds to the methylene protons (THF and ECH) adjacent to the oxygen atom. We can also observe the protons of the methyl group CH_3 of acetic anhydride at 2 ppm. This last signal prove the fixation of acetyl ($COCH_3$) in chain end.

For a preview on the structure of the copolymer, IRFT spectra (figure 2) of the copolymers were recorded. Firstly, we observe the disappearance of the characteristic band of the epoxy function located between 890 and 900 cm-1. This is evidence that the polymerization takes place by ring opening. All copolymers show absorption bands between 2798-2939 cm-1 and 1082-1113 cm-1 corresponding, respectively to stretching vibrations of aliphatic C–H of the methylene and to the C–O–C stretching vibration. Finally, all copolymers show absorption at around 1739 cm^{-1} assigned to stretching vibrations of carbonyl of chain end.

The results in figure 3 clearly indicate that an optimal rate of reaction is obtained at room temperature by copolymerizing ECH in bulk with Mag-H$^+$ proportion equal to 10 %. Under these conditions, monomer conversion reaches 45 % after 20min.This finding is in good agreement with the proposal that Mag-H$^+$ is present as the active initiator species since the number of those species should be related to their surface area. Similar results are obtained by Njopwouo et al (6).

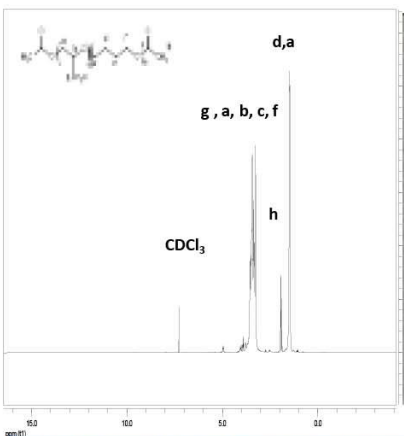

Fig. 1.^{1}H NMR spectrum of poly(THF-ECH) product of the reaction presence of AC

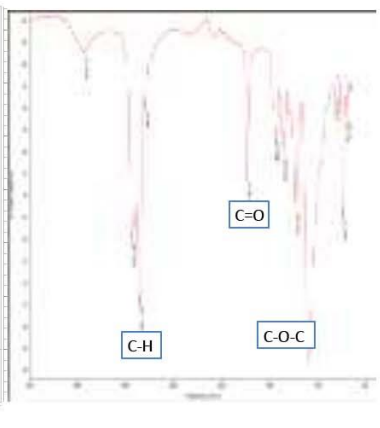

Fig.2. FT-IR spectrum of poly(THF-ECH) in the

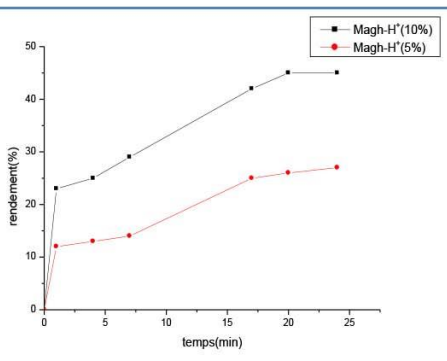

Fig. 3. Conversions with time for 8.2g of THF, 6.2 g of ECH the amounts of Mag-H$^+$ 0.25M were: , a)5% , b)10%

Conclusions

Maghnite-H+, proton exchanged montmorillonite clay can catalyze a variety of polymeric reactions occurring on their surface and interstitial space. In the copolymerization of cyclic ethers, the solid catalyst was thought to act as an acid to generate cation species. Actually, the efficiency of the copolymerization reflected the Lewis acidity of Maghnite-H+.

Several main advantages were shown in the transformation system, the copolymer was produced by a very simple procedure, just by filtering, the clay can be separated from the reaction mixtures, modified clay is inexpensive, stable, non corrosive and recycled without a loss of catalytic activity.

References

1. Jaiswal , S et al . International Journal on Cybernetics & Informatics (IJCI) Vol. 6, No.1/2, April (2017).

2. Kaur, N and Kishore, D. Journal of Chemical and Pharmaceutical Research, 4(2):991(1015) (2012)

3. Araf S.D et al . The Open Macromolecules Journal, 2, 54-57(2008).

4. Belbachir, M. U.S. Pat. 066969.0101 (2001).

5. Hamilton , S.C and Semlyen ,J.A. *Polymer*, 38, 1685-1691(1997).

6. Njopwouo ,D ; Roques ,G and Wandji, R. *Clay Minerals*, 22 (1), 145-156 (1987).

SYNTHESIS OF SOME NEW 2-PHENOXYACETAMIDE AND 3-PHENOXYPROPANAMIDE DERIVATIVES AND EVALUATION OF THEIR CHOLINESTERASE INHIBITOR ACTIVITIES

Shakıla Shakıla [a]*, Burcu Kılıç[a], Fatma Aksakal [b], Deniz S. Doğruer[a]

[a] Department of Pharmaceutical Chemistry, Gazi University Faculty of Pharmacy, Ankara, Turkey

[b] Department of Chemistry, Hacettepe University, Ankara, Turkey

shaks977@gmail.com

INTRODUCTION

Alzheimer's disease (AD) is a chronic neurodegenerative brain disease that affects the elderly. It accounts for more than half of all dementia cases. According to the 2019 report of Alzheimer Disease International, there are approximately 50 million people living with dementia worldwide, and the disease's prevalence will triple by 2050 due to a rise in average life expectancy [1]. Although extensive research has been focused on pathogenetic mechanism of AD, the exact cause of it is still uncertain. Several hypotheses have been proposed as the cause of AD. One of them is cholinergic hypothesis which states the main cause of AD is the reduction in acetylcholine (ACh) level. Therefore, one of the potential therapeutic strategies is to increase the acetylcholine's level in brain by inhibiting the activity of cholinesterase enzymes [2].

In the present study, we designed and synthesized 2-phenoxyacetamide and 3-phenoxypropanamide derivatives in order to investigate their acetylcholinesterase/butyrylcholinesterase inhibitory activities.

MOLECULAR DOCKING

The docking studies of most active compounds were performed to predict the binding conformations and non-covalent interactions with the active sites of the AChE and BChE. Herein, the docking results of compound **1** and **3** with BChE and AChE enzymes respectively are presented in Fig 1.

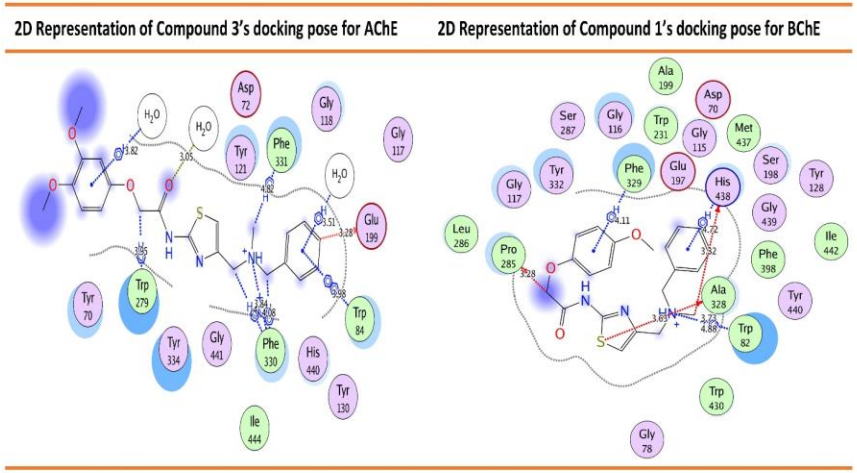

Fig 1. 2D Representation of docked poses for the compounds 1 and 3 in the active sites of BChE and AChE.

ACKNOWLEDGEMENTS

This work was supported by the Scientific and Technological Research Council of Turkey (TUBITAK) [grant number 118S686].

CHEMISTRY

In this study, 5 new compounds were synthesized according to following scheme and their structures were confirmed by ^{1}H-NMR, ^{13}C NMR, HRMS, and elemental analysis. The ^{1}H NMR, ^{13}C NMR, mass spectra and elemental analysis data of the compounds were consistent with the proposed structures.

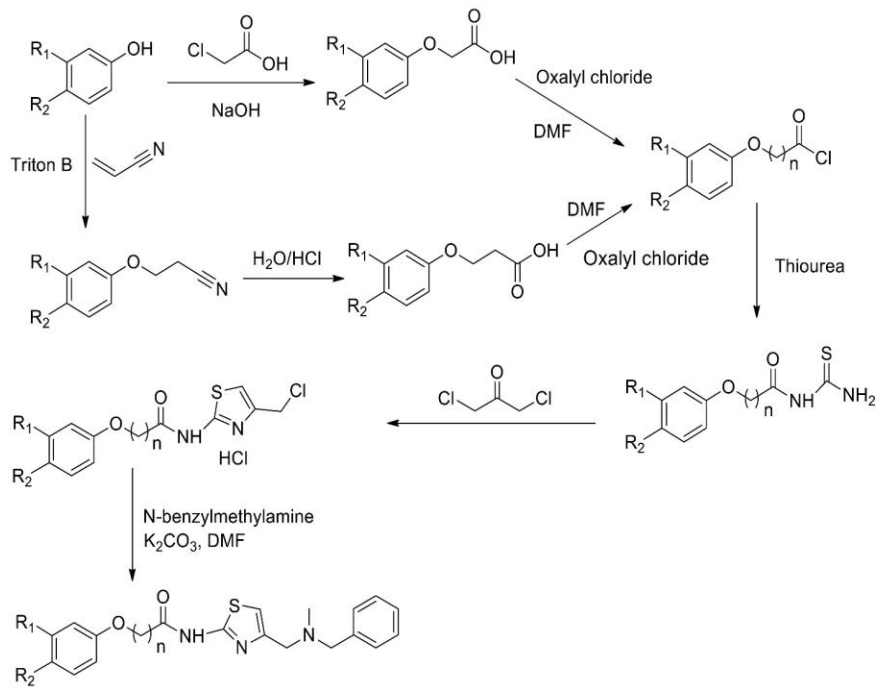

Fig 2. Synthetic scheme route of the synthesized compounds

BIOLOGICAL STUDIES

AChE and BuChE inhibitory activities of the test compounds at 10 µM concentration and their IC_{50} values were determined by the modified Ellman's method [3]. Electric eel AChE (type-VI-S, EC 3.1.1.7, Sigma) and equine serum BuChE (EC 3.1.1.8, Sigma) were employed as the enzyme sources.

Compound	n	R_1	R_2	AChE		BChE	
				%inh± SD (10µM)	IC_{50} (µM) ± SD	%inh± SD (10µM)	IC_{50} (µM) ± SD
1	1	OCH_3	H	53 ± 0.3	12.10 ±0.02	84 ± 0.04	2.10 ± 0.09
2	1	CH_3	H	19 ± 5.2	≥20	82 ± 0.3	2.86 ± 0.05
3	1	OCH_3	OCH_3	68 ± 3.3	5.80 ±0.12	53 ± 4.2	12.39± 0.07
4	2	OCH_3	H	55 ± 4.9	12 ± 0.05	67 ± 1.7	5.64 ± 0.06
5	2	CH_3	H	27 ± 4.2	≥20	72 ± 3.4	4.99 ± 0.08
Donepezil				98 ± 1.0	0.058 ±0.01	90 ± 0.5	3.7 ± 0.02

Table 1. Cholinesterase inhibitory activities of the synthesized compounds.

DISCUSSION

In conclusion, a series of 2-phenoxyacetamide and 3-phenoxypropanamide derivatives have been designed, synthesized and evaluated as ChE inhibitors. According to the cholinesterase inhibitory activity results, synthesized compounds generally exhibited prominent BChE inhibitory activity except for compound **3** which exhibited greater AChE inhibitory activity than BChE inhibitory activity. Among the synthesized compounds, compound **1** was the most active one in terms of BChE inhibitory activity. Further studies for determination of metal chelation properties and anti-inflammotory activities of synthesized compounds are under ongoing investigation in our laboratory.

REFERENCES

[1]. International, A.s.D., World Alzheimer Report 2019 Attitudes to dementia 2019.

[2]. Stanciu, G.D., et al., Alzheimer's Disease Pharmacotherapy in Relation to Cholinergic System Involvement. Biomolecules, 2019. **10**(1).

[3]. Erdogan M, Kilic B, Sagkan RI, Aksakal F, Ercetin T, Gulcan HO, Dogruer DS. Design, synthesis and biological evaluation of new benzoxazolone/benzothiazolone derivatives as multi-target agents against Alzheimer's disease. European Journal of Medicinal Chemistry. 2021 Feb 15;212:113124.

13th International Symposium on Pharmaceutical Sciences (ISOPS) 22-25 June 2021.ANKARA,TURKEY

SYNTHESIS AND IN VITRO EVALUATION OF THE ANTIOXIDANT ACTIVITY OF IMINES.

Faïza Memmou[1,*], Houcine Benmehdi[2], Assia Tounsi[1], Fellah Khadidja[2].
[1]Department of Material Sciences, Faculty of Exact Sciences, University of Tahri Mohamed-Bechar, B.P. 417, Bechar, Algeria.
[2]Laboratory of Chemistry and Environmental Sciences, Department of Biology, University of Tahri Mohamed-Bechar, B.P. 417, Bechar, Algeria
*Corresponding author: E-mail: Fmemmou2002@yahoo.fr

Abstract
This work is part of the imines synthesis and their valorization as antioxidants. We performed several tasks divided into two parts: The first part is to realize the synthesis of imines (Schiff bases). Products *(E)*-4-((2-aminoéthylimino)méthyl)-2-méthoxyphénol and 4,4'-((1*E, 1'E)*-(éthane-1,2-diylbis (azanylylidéne)) bis (méthanylylidéne)) bis (2-méthoxyphénol) been obtained with quantitative yields. In the second part, the synthesized products have been subjected to a biological evaluation in terms of antioxidant activity via the use of two techniques: the qualitative bioautographic test (HPTLC) and a quantitative test (2,2-diphenyl-1-picrylhydrazyl (DPPH•) radical scavenging method). It has been found that imines revealed the positive reaction (yellow spots) on the TLC plates sprayed with DPPH• methanol solution. The DPPH• antioxidant test of the products in question allowed us to measure the IC50 inhibition concentration. The results show that the imines proved to be the most effective with an IC 50 of the order of 0.77 mg / mL; 0.42 mg / mL respectively.
Key words: synthesis, imines, antioxidant activity, HPTLC, DPPH •

Introduction

In recent years, researchers have been interested in the preparation of imines (Schiff's bases) by different methods, for differences in medical, biological, and other reactivities that they present. They use antibiotic, antibacterial, anti-cancer, anti-tumor, anti-tuberculosis and several incurable diseases. Imines (Schiff bases) are defined as chemicals containing one or more imine groups (-C = N). They are widely used in medicine for the treatment of several diseases and in industry, in the fight against corrosion, for example **[1].**
The antioxidant activity of a compound is its ability to resist oxidation. The most known antioxidants are β-carotene (provitamin A), ascorbic acid (vitamin C), tocopherol (vitamin E) and phenolic compounds. Indeed, most of the synthetic or naturally occurring antioxidants have hydroxyphenolic groups in their structures and the antioxidant properties are attributed in part to the ability of these natural compounds to trap free radicals such as hydroxyl radicals(OH•) and superoxides (O2•) . Several methods are used to evaluate, in vitro and in vivo, the antioxidant activity by trapping different radicals, such as peroxides ROO • by the ORAC(Oxygen Radical Absorbance Capacity) and TRAP (Total Radical-Trapping Antioxidant Parameter) methods ; ferric ions by the FRAP method (Ferric ion Reducing Antioxidant Parameter) or the ABTS• radicals, as well as the method using the free radical DPPH• (diphenyl-picrylhydrazyl) **[2].**

Objectifs

The objective of our work is to develop methods for the synthesis of new organic molecules (imines). Establish structure-property relationships of synthesized organic molecules (in vitro test of antioxidant activity by several methods DPPH•).

Materials and Methods:

PART I: Synthesis of imines

L1 ligand is obtained by condensation of a vanillin molecule with a diamine molecule in the presence of ethanol in the form of solids (**Scheme 1**).On the other hand, ligand L2 is obtained by condensation of two vanillin moleculeswith a diamine molecule in the presence of ethanol in the form of solids (**Scheme 2**).

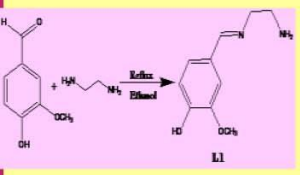

Scheme 1*: Synthesis of ligand L1.*

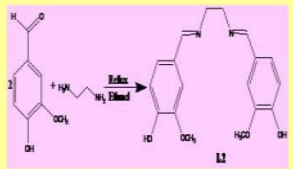

Scheme 2 *: Synthesis of ligand L2.*

PART II: Antioxidant activity

DPPH radical scavenging activity

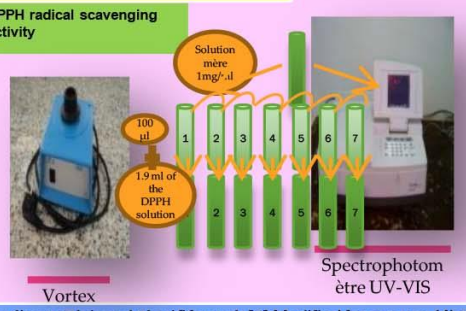

According to Blois and Sharififar et al. [5] Modified for our use **(4)**.Free radical inhibition DPPH (% DPPH) is calculated as follows:
I%= [(Abs control – Abs products) /Abs control] × 100
With: Abs control: absorbance of DPPH
Abs products: product absorbance
The values of the IC50 have been determined graphically (**Figure 1**).

Results and discussion

PART I: Synthesis of imines

☛ The ligands L1 and L2 are obtained by condensation of one or two molecules of vanillin with one molecule of diamine in the presence of ethanol in the form of solids.The products L1 [*(E)*-4-((2-aminoéthylimino)méthyl)-2-méthoxyphénol] and L2 [4,4'-((1*E,* 1'*E)*-(éthane-1,2-diylbis (azanylylidéne)) bis (méthanylylidéne)) bis (2-méthoxyphénol) were isolated after 2h of cooling reflux, with quantitative yields for of the order of 66 % ; 77 %respectively . The purity of these products was confirmed by chromatography (TLC) and characterized by their IR and 1H and 13C NMR spectra.

PART II: Antioxidant activity

DPPH radical scavenging activity

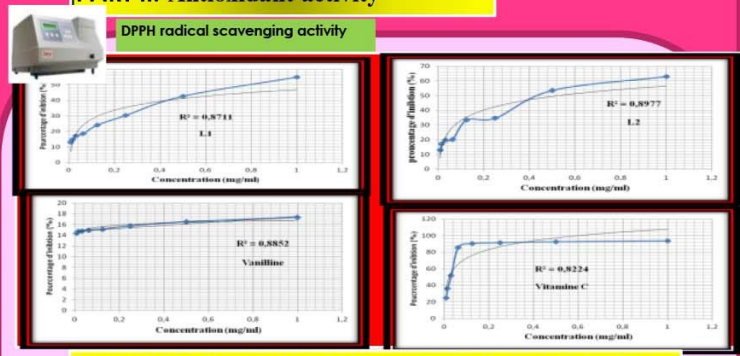

Figure 1: Variation of the percentage of inhibition as a function of the concentrations of the synthesized products

☛ In order to confirm the antioxidant power of our products, we have deduced the IC50 values from the curves % I = f (C).From these results, ascorbic acid is most effective with an IC50 of 0.03 mg / mL compared to synthesized products L1 and L2 .The DPPH• antioxidant test of the products in question allowed us to measure the IC50 inhibition concentration. The results show that the imines proved to be the most effective with an IC 50 of the order of 0.77 mg / mL; 0.42 mg / mL respectively.
IC50 values for products synthesized in the presence of ascorbic acid are summarized in **Table 2** and **Figure 2**:

Synthesized products	IC 50 (mg/mL)
L_1	0.77
L_2	0.42
Ascorbic acid	0.030
Vanillin	0

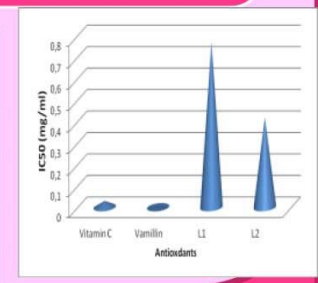

Conclusions

According to the results obtained we can say that our products have an antioxidant activity in vitro with the DPPH• method.

Références

[1] Université de Fribourg , «Campus virtuel suisse (SVC) Programme fédéral d'impulsion» , Chimie générale, campus virtuel suisse (CVS), Copyright, **2005**.
[2] C. Popovici, I.Saykova , B.Tylkowski. Evaluation de l'activité antioxydant des composés phénoliques par la réactivité avec le radical libre DPPH. *Revue de génie industriel* .2009, 4, 25-39.
[3] K.H.Chjo, B.G.Jeong, J.H.Kim, S.Jeon, C.P.Rym et Y.K.Choi .*Bull Korean Chem Soc.***1997**.18 (8) ,850
[4] R. Mahboub, F.Memmou. Antioxidant activity and kinetics studies of eugenol and 6-bromoeugenol. *Natural product research.***2014.**
[5] F. Sharififar, M.H.Moshafi, S.H.Mansouri, M .Khoshnoodi. In vitro evaluation of antibacterial and anitoxydant activities of the essential oil and methanol extract of endemic Zataria multiflora Boiss .*Food Control* .**2007**. 18.800-805.

JUNE 22-25, 2021 ANKARA, TURKEY
13th International Symposium on Pharmaceutical Sciences

SYNTHESIS AND STANDARDIZATION OF AN IMPURITY OF ACETAMINOPHEN, DEVELOPMENT AND VALIDATION OF RELATED ULTRA-HIGH PERFORMANCE LIQUID CHROMATOGRAPHIC METHOD

Cemil Caner Arıkan[1], İlkay Küçükgüzel[2]

[1] Atabay Pharmaceuticals and Fine Chemicals Inc., Acıbadem Plant and Headquarters, Kadıköy 34718 İstanbul, Turkey
[2] Marmara University, Faculty of Pharmacy, Department of Pharmaceutical Chemistry, Haydarpaşa 34668 İstanbul, Turkey
canerarikan@marun.edu.tr

Introduction

Acetaminophen (*N*-(4-Hydroxyphenyl)acetamide) also known as paracetamol is a common analgesic and antipyretic drug used for the relief of fever, aches and pains [1,2]. When acetaminophen is analyzed by HPLC according to organic impurities analysis method of acetaminophen in American Pharmacopoeia Version 42 (USP 42) [3], an impurity molecule is observed on the chromatogram which is not defined by the USP 42. We identified this impurity molecule as N,N'-[Oxydi(4,1-phenylene)]diacetamide (ODAA) by LC-MS/MS and other studies. In the present work, this molecule was synthesized, characterized, standardized and the current HPLC method for organic impurities analysis of acetaminophen was transferred to UHPLC by developing a new related method including this impurity. The method was validated according to international conference on harmonization (ICH) guideline [4] and stress-test studies of acetaminophen were performed with forced degradation studies.

Methods | Synthesis and Characterization

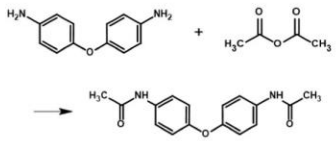

Figure 1: Synthesis of ODAA.

- **Yield:** 95%
- **Melting Point:** 230°C.
- **Appearance:** White crystalline powder.
- **Solubility:** Soluble in ethanol, methanol and DMSO.

Table 1: Elemental analysis of ODAA.

Element	Amount by mass (%)	
	Calculated	Found
Carbon (C)	67.590	66.890
Hydrogen (H)	5.670	5.582
Nitrogen (N)	9.850	9.849

N,N'-[Oxydi(4,1-phenylene)]diacetamide (ODAA) was synthesized by dissolving 4,4'-Oxydianiline in acetone at 0°C and adding acetic anhydride dropwise and the reaction was carried out for 3h at 0°C. For crystallisation, the obtained ODAA was completely dissolved in ethanol and the final solution was evaporated. The synthesized ODAA was identified by the use of IR, ^{1}H-NMR, ^{13}C-NMR, IIMBC NMR, IIPLC, LC-MS/MS, elemental analysis and melting point determination.

Table 2: NMR results of ODAA.

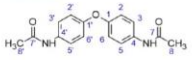

No	^{1}H-NMR	^{13}C-NMR	^{1}H-^{13}C Interactions	^{13}C-^{1}H Interactions
8,8'	2,032	24,32	7, 7', 8*, 8'*	8*, 8'*
1, 1'	-	152,79	-	2, 3, 5, 6, 2', 3', 5', 6'
2, 6, 2', 6'	6,92-6,94	119,07	1, 2*, 3, 4, 5, 6*, 1', 2'*, 3', 4', 5', 6'*	2*, 3, 5, 6*, 2'*, 3', 5', 6'*
3, 5, 3', 5'	7,55-7,58	121,08	1, 2, 3*, 4, 5*, 6, 1', 2', 3'*, 4', 5'*, 6'	2, 3*, 5*, 6, 2', 3'*, 5'*, 6', NH
4, 4'	-	135,32	-	2, 3, 5, 6, 2', 3', 5', 6', NH
NH	9,93	-	3, 4, 5, 7, 3', 4', 5', 7'	-
7, 7'	-	168,47	-	8, 8', NH

Q3 Scan Mode

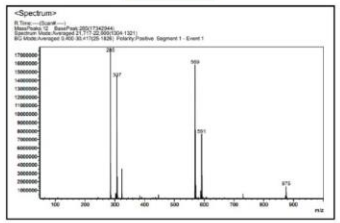

- 285 m/z: ODAA + 1H (284+1= 285 g/mol)
- 307 m/z: ODAA + Na (284+23= 307 g/mol)
- 569 m/z: ODAA dimer ((284x2)+1H= 569 g/mol)
- 591 m/z: ODAA dimer + Na ((284x2)+23= 591 g/mol)
- 875 m/z: ODAA trimer+ Na ((284x3)+23= 875 g/mol)

Product ion scan of 285 m/z

Product Ion Scan Mode

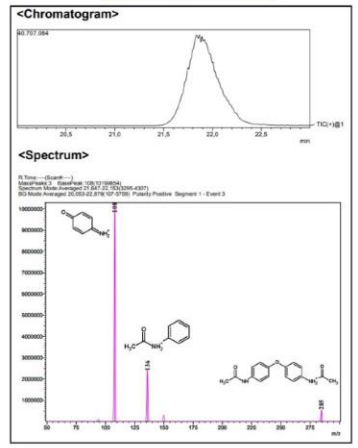

Figure 2: Results of LC-MS/MS.

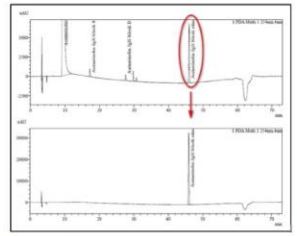

Figure 3: IIPLC chromatograms of acetaminophen sample solution and ODAA solution.

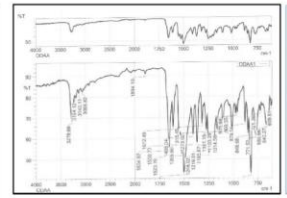

Figure 4: IR spectrum of ODAA.

$\bar{\nu}_{max.}$ (cm^{-1}):

- 3279 (N-H s.)
- 3194 ve 3140 (aromatic C-H s.)
- 3067 (aliphatic C-H s.),
- 1655 (C=O s.)
- 1612 (aromatic C=C s.)
- 1551 (N-H b.)
- 1500 (C-H asymmetric b.)
- 1366 ve 1315 (C-H symmetric b.)

s. : stretching
b. : bending

Standardization of ODAA

➢ The potency of the synthesized ODAA molecule was calculated with the help of the following formula [5] and the results found in Table 3:

Table 3: Results for calculating the potecy of ODAA.

Analysis	Method	Results
Organic Impurities	HPLC	%0,010000
Inorganic Impurities	Residue on Ignition (Sulfated Ash)	%0,009946
Residual Solvents	GC	%0,037027
Water Content	Karl Fischer	%0,305000

$$\text{Potency (\%)} = 100\% \times \frac{100\% - \%\ \text{impurities}}{100} \times \frac{100\% - [\%\ \text{water} + \%\ \text{residual solvents} + \%\ \text{others}]}{100}$$

$$\text{Potency (\%)} = 100\% \times \frac{100\% - 0{,}01\%}{100} \times \frac{100\% - [0{,}305\% + 0{,}037027\% + 0{,}009946\%]}{100}$$

➢ The potency of the synthesized ODAA molecule was calculated using the results above and found to be **99.64%**.

UHPLC Method Development

➢ Method development studies were performed on the Shimadzu Nexera X2 model ultra-high performance liquid chromatography (UHPLC) system equipped with a photodiode array detector.

Table 4: Chromatographic system conditions for the UIIPLC system.

Chromatography	Ultra-High Performance Liquid Chromatography (UHPLC)
Detector	UV 254 nm
Column	InertSustain C8, 150 × 2,1 mm, 2-µm
Flow	0,2 mL/min.
Column Temperature	40°C
Injection Volume	1 µL
Run Time	30 min.

Table 5: Mobile phase program for gradient elution (UHPLC).

Time (min.)	Solvent A (%)	Solvent B (%)
0	65	35
1	65	35
6	22	78
22	22	78
23	65	35
30	65	35

Solvent A: Methanol, water, glacial acetic acid (50:950:1, v/v/v)
Solvent B: Methanol, water, glacial acetic acid (500:500:1, v/v/v)
Diluent: Methanol

Validation

Table 6: System suitability results of the UHPLC method.

Substance	Tailing Factor (T)	Resolution (R)	RSD %
Acetaminophen	1.203	-	0.429
Acetaminophen related compound B	1.093	12.302[a]	0.448
Acetaminophen related compound C	1.063	2.825[b]	0.433
Acetaminophen related compound D	1.038	-	0.414
Acetaminophen related compound J	1.013	-	0.918
ODAA	1.037	2.454[c]	0.421
Required limits	T ≤ 2.0	a: ≥ 2.0; b: ≥ 1.5; c ≥ 1.5;	RSD ≤ 5.0 %

Table 7: Acetaminophen impurity limits and specificity results of the UHPLC method.

Substance	Limit (max. %)	Retention Time (RT) (min)	Relative Retention Time (RRT)	Peak Purity Index	Single Point Threshold
Acetaminophen	-	4.492	1.000	1.0000	0.941500
Acetaminophen related compound B	0.050	7.339	1.634	1.0000	0.789221
Acetaminophen related compound C	0.050	8.061	1.795	1.0000	0.870031
Acetaminophen related compound D	0.050	11.881	2.645	1.0000	0.956029
Acetaminophen related compound J	0.001	20.649	4.597	1.0000	0.835209
ODAA	0.050	21.533	4.794	1.0000	0.918711

Table 8: Precision results of the UIIPLC method.

Substance	System Precision		Method Precision	
	RSD % (Peak areas, n=6)	RSD % (Retention times, n=6)	Amount % (n=6)	RSD % (n=6)
Acetaminophen	0.429	0.063	-	-
Acetaminophen related compound B	0.448	0.069	0.04994	0.472
Acetaminophen related compound C	0.433	0.052	0.04628	0.667
Acetaminophen related compound D	0.414	0.050	0.04804	0.529
Acetaminophen related compound J	0.918	0.053	0.00102	1.257
ODAA	0.421	0.068	0.04943	0.563

Table 10: Results of regression analysis of the linearity data of acetaminophen and its impurities.

Substance	Range (µg/mL)	Slope	Intercept	r^2	LOD (µg/mL)	LOQ (µg/mL)
Acetaminophen	1.248 - 24.960	18082420	4345.691	0.9998	0.374	1.248
Acetaminophen related compound B	0.373 - 24.885	13226230	415.7887	0.9994	0.124	0.373
Acetaminophen related compound C	1.217 - 24.347	6015866	324.0392	1.0000	0.365	1.217
Acetaminophen related compound D	0.369 - 24.611	15230310	703.6019	1.0000	0.123	0.369
Acetaminophen related compound J	0.125 - 0.499	26382500	-88.31898	0.9999	0.050	0.125
ODAA	0.373 - 24.850	33323090	665.3543	0.9983	0.124	0.373

Table 12: Degradation results of acetaminophen.

Stress condition	Time (day)	% Assay of the impurities						
		Imp-B*	Imp-C*	Imp-D*	Imp-J*	ODAA	Total degradation impurities	Total impurities
Acidic hydrolysis (1.0 N HCl)	0	0.0018	ND	ND	ND	≤ LOQ	-	0.0018
	1	0.0017	ND	ND	ND	≤ LOQ	0.0564	0.0581
	15	≤ LOQ	ND	ND	ND	≤ LOQ	0.7621	0.7621
Alkaline hydrolysis (1.0 N NaOH)	0	0.0018	ND	ND	ND	≤ LOQ	-	0.0018
	1	0.0030	ND	ND	ND	≤ LOQ	0.3878	0.3906
	15	0.0033	ND	ND	ND	≤ LOQ	0.8487	0.8520
Oxidation degradation (3.0% H_2O_2)	0	0.0018	ND	ND	ND	≤ LOQ	-	0.0018
	1	0.0018	ND	ND	ND	≤ LOQ	≤ LOQ	0.0018
	15	0.0020	ND	ND	ND	≤ LOQ	0.0154	0.0174
Thermal degradation (Dry heat, 60°C ± 2°C	0	0.0018	ND	ND	ND	≤ LOQ	-	0.0018
	1	0.0018	ND	ND	ND	≤ LOQ	≤ LOQ	0.0018
	15	0.0020	ND	ND	ND	≤ LOQ	≤ LOQ	0.0020
Photolytic degradation (UV light, 254 nm)	0	0.0018	ND	ND	ND	≤ LOQ	-	0.0018
	1	0.0019	ND	ND	ND	≤ LOQ	≤ LOQ	0.0019
	15	0.0019	ND	ND	ND	≤ LOQ	≤ LOQ	0.0019

*: Imp-B: Acetaminophen related compound B, Imp-C: Acetaminophen related compound C, Imp-D: Acetaminophen related compound D, Imp-J: Acetaminophen related compound J; ND: not detected

Table 9: Accuracy results of the UIIPLC method.

Substance	Concentration (µg/mL) (n=3)	Recovery (%)	RSD (%)
	Theoretical	Found	(n=3)	(n=3)
50% Level of the limit concentration				
Acetaminophen related compound B	6.2213	6.2559	100.56	0.284
Acetaminophen related compound C	6.0868	5.7033	94.69	0.282
Acetaminophen related compound D	6.1529	5.7705	93.79	0.348
Acetaminophen related compound J	0.1241	0.1206	97.18	2.036
ODAA	6.2126	5.8907	94.82	0.234
100% Level of the limit concentration				
Acetaminophen related compound B	12.4426	12.4698	100.22	0.959
Acetaminophen related compound C	12.1735	11.7620	96.62	0.464
Acetaminophen related compound D	12.3057	11.9742	97.31	0.728
Acetaminophen related compound J	0.2482	0.2557	103.02	0.432
ODAA	12.4251	12.3578	99.46	0.861
150% Level of the limit concentration				
Acetaminophen related compound B	18.6639	19.1014	102.34	1.144
Acetaminophen related compound C	18.2603	17.6591	96.71	0.732
Acetaminophen related compound D	18.4586	17.8973	96.96	1.124
Acetaminophen related compound J	0.3723	0.3620	97.23	1.300
ODAA	18.6377	18.1341	97.30	1.234

Table 11: Robustness results of the UIIPLC method.

Substance	RSD %		RSD %	
	λ = 252 nm	λ = 256 nm	T = 35°C	T = 45°C
Acetaminophen related compound B	0.514	2.493	1.571	0.162
Acetaminophen related compound C	1.216	2.616	2.951	3.559
Acetaminophen related compound D	0.291	3.477	2.250	0.656
Acetaminophen related compound J	0.965	2.882	0.992	1.210
ODAA	0.686	3.683	2.288	0.568

➢ Solution stability test was also performed during validation studies for both reference solution and test solution spiked with impurities at the specification limits.

➢ Solution stability test demonstrated that the reference and the test solution prepared within the developed UIIPLC method showed a minimum of 24h solution stability.

Results and Discussion

An undefined impurity molecule of acetaminophen in USP 42 was synthesized, characterized, standardized and an UHPLC method including this impurity was developed for the analysis of organic impurities of acetaminophen. Requirements for the validation study of the developed method were fulfilled according to ICH. The validated UHPLC method has been proved to be sensitive, selective, specific, precise, linear, accurate and robust. The developed method provides a good resolution between acetaminophen, acetaminophen related compound B, acetaminophen related compound C, acetaminophen related compound D, acetaminophen related compound J and ODAA, and could be used for determination of organic impurities of acetaminophen. Compared to the related method in USP 42, the new developed UHPLC method offers a short analysis time and uses less mobile phase.

Acknowlegements

The authors are thankful to Marmara University, Faculty of Pharmacy, Department of Pharmaceutical Chemistry, Istanbul, Turkey and Atabay Pharmaceuticals and Fine Chemicals, Istanbul, Turkey, for letting use of their laboratories, chemicals and instruments.

References

1. M. Espinosa Bosch, A.J. Ruiz Sánchez, F. Sánchez Rojas, C. Bosch Ojeda, Determination of paracetamol: Historical evolution, J. Pharm. Biomed. Anal. 42 (2006) 291–321.
2. M.J. O'Neil (ed.), The Merck Index: An encyclopedia of chemicals, drugs, and biologicals, 13th ed. (2001), Merck and Co., Inc., Whitehouse Station, New Jersey, USA.
3. United States Pharmacopeia 42. Volume 1. Official Monographs: Acetaminophen. United States Pharmacopeial Convention, 12601, Twinbrook Parkway, Rockville, MD 20852. 2020; p:40-42.
4. ICH Topic Q2 (R1): Validation of Analytical Procedures: Text and Methodology. Step 5. Note For Guidance On Validation of Analytical Procedures: Text And Methodology. CPMP/ICH/381/95. European Medicines Agency, 1995.
5. D.K. Singh, S. Sharma, A. Thakur, S. Kumar, S. Singh, Pharmaceutical analysis - Drug purity determination. In: P. Worsfold, A. Townshend, C. Poole, M. Miró, eds. Encyclopedia of Analytical Science. 3rd ed. Elsevier Ltd. (2019) 188-199.

IN SILICO DESIGN AND SYNTHESIS OF NOVEL 2-ACYLHYDRAZONO-5-ARYLMETHYLENE-4-THIAZOLIDINONES AS ENOYL-ACYL CARRIER PROTEIN REDUCTASE INHIBITORS

[1] Serap İpek DİNGİŞ BİRGÜL, [1] İlkay KÜÇÜKGÜZEL, [2] Atilla AKDEMİR

[1] Marmara University, Department of Pharmaceutical Chemistry, Istanbul, Turkey, ipekdingis@gmail.com, ikucukguzel@marmara.edu.tr

[2] Bezmialem Vakif University, Computer-aided Drug Discovery Laboratory, Department of Pharmacology, Istanbul, Turkey, aakdemir@bezmialem.edu.tr

INTRODUCTION

The synthesis of mycolic acid, which is the essential component of mycobacterial cell wall, is controlled by two systems: fatty acid synthase system type-1 (FAS-I) and fatty acid synthase system type-2 (FAS-II). Since eukaryatic cells produce fatty acids using only the FAS-I enzyme system, the FAS-II enzyme system can be an appropriate target for selective antimycobacterial drugs (1). The FAS-II pathway, which consists of the enoyl-acyl carrier protein reductase enzyme (InhA) (2), is a validated target for antimycobacterial drugs. Within the scope of this work, compounds with high binding affinity were selected, synthesized and their structures were elucidated.

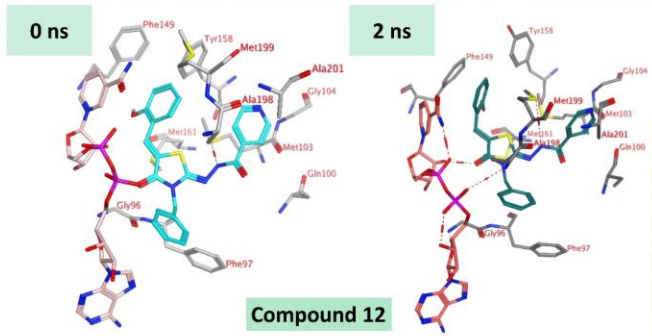

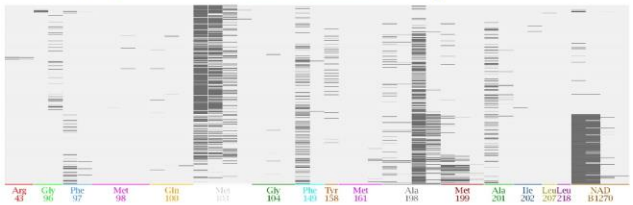

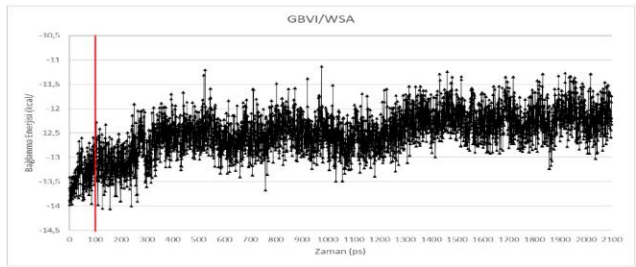

DISCUSSION

The crystal structures obtained from the RCSB-Protein Data Bank (PDB) were examined and 3 crystal structures (PDB: 4TZK, 4BQP, 4BGE) were selected for use in molecular modeling and dynamics studies. The 4BGE crystal structure was chosen to identify hits that could bind without a cofactor (NAD). The reason for choosing two crystal structures containing cofactor is that the amino acids Tyr158, Ile215, Ile202, Met103 and Leu207 in the binding region show different conformations. These differences can lead to variation in poses in the hydrophobic region. After the validation studies, the database containing approximately 15,000 molecules was screened against the mentioned crystal structures. Molecular dynamics studies were performed using NAMD software package (v2.12, Theoretical and Computational Biophysics Group, NIH Center for Macromolecular Modeling and Bioinformatics, The Beckman Institute, University of Illinois at Urbana-Champaign) for the original ligands of the crystal structures and the suggested ligands as a result of molecular docking analysis. In the light of all these studies, the synthesis of 22 molecules predicted to bind to the enzyme was carried out. Due to the low synthesis efficiency of thiazolidin-4-one compounds, triethyl amine was used as a base instead of sodium acetate, unlike what is reported in the literature.

MATERIALS AND METHODS

Virtual screenings and molecular dynamic simulation (MD) studies were performed on a proprietary library using the MOE (version 2020.04, chemical computing group, Inc., Montreal, Canada), FlexX (LeadIT, version 4.1, BioSolveIT GmbH, Sankt Augustin, Germany, 2019) and NAMD (v2.12, Theoretical and Computational Biophysics Group, NIH Center for Macromolecular Modeling and Bioinformatics, The Beckman Institute, University of Illinois at Urbana-Champaign) software packages. Subsequently, synthesis of selected compounds were performed. N-substituted thiosemicarbazides were obtained from benzoic acid, nicotinic acid and isonicotinic acid hydrazides (4,5). These thiosemicarbazides were cyclized in ethanolic medium containing triethyl amine by the addition of ethyl bromoacetate to achieve N-substituted thiazolidin-4-one compounds (5). The final products bearing the 5-arylidene group were obtained by the reaction of these rings with various aldehydes in methanolic sodium methoxide (5). The structural characterization of all molecules were determined by IR, 1H-NMR and mass spectroscopy. Their purity was checked by TLC and HPLC studies.

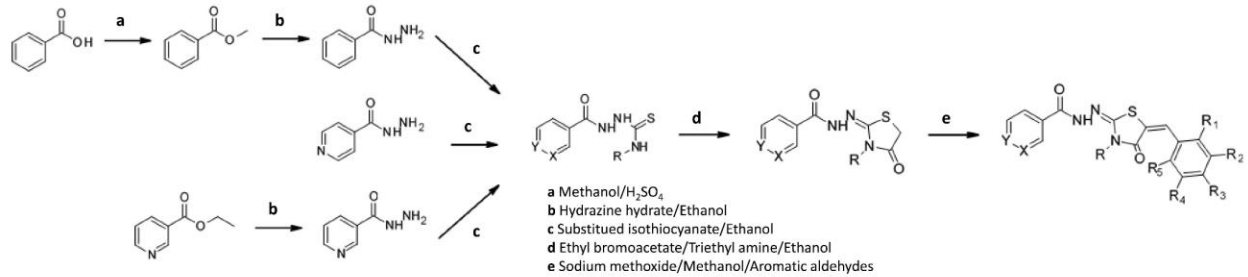

a Methanol/H_2SO_4
b Hydrazine hydrate/Ethanol
c Substitued isothiocyanate/Ethanol
d Ethyl bromoacetate/Triethyl amine/Ethanol
e Sodium methoxide/Methanol/Aromatic aldehydes

	IR(cm^{-1})	^{1}H-NMR (400 MHz) (DMSO-d_6/TMS) δ ppm	Mass (calculated m/z / found Da)
Compound 1	3140 (N-H s.b.); 3043 (aromatic C-H s.b.); 2978, 2939 (aliphatic C-H s.b.); 1705, 1639 (C=O s.b.); 1612 (C=N s.b.)	1.28 (t, 3H, J_1= 6.8 Hz, J_2= 7.2 Hz, CH_2-CH_3); 3.95 (q, 2H, J_1=6.8 Hz, J_2=7.2 Hz, CH_2-CH_3); 7.44-8.03 (m, 11H, =C*H*-Ar, Ar-*H*); 11.23 (s, 1H, N*H*-N)	APCI$^+$ ([M+H]$^+$), 352,11 / 352,20
Compound 2	3147 (N-H s.b.); 3070, 3020 (aromatic C-H s.b.); 2978, 2939 (aliphatic C-H s.b.); 1705, 1647 (C=O s.b.); 1620, 1604 (C=N s.b., C=C s.b.)	1.28 (t, 3H, J_1= 7.2 Hz, J_2= 7.2 Hz, CH_2-CH_3); 3.95 (q, 2H, J_1=6.8 Hz, J_2=7.2 Hz, CH_2-CH_3); 7.32-7.91 (m, 10H, =C*H*-Ar, Ar-H); 11.24 (s, 1H, N*H*-N)	APCI$^-$ ([M-H]$^-$), 368,08 /368,15
Compound 3	3197 (N-H s.b.); 3066, 2974 (aromatic C-H s.b.); 2935 (aliphatic C-H s.b.); 1705, 1651 (C=O s.b.); 1600, 1577 (C=N s.b., C=C s.b.)	4.54 (s, 2H, N-CH_2-CH-); 5.24 (d, 2H, J=8.8 Hz, -CH=CH_2); 5.97 (m, 1H, CH_2-CH=CH_2); 7.39 – 7.91 (m, 10H, Ar-*H*, =C*H*-Ar); 11.27 (s, 1H, N*H*-N)	APCI$^+$ ([M+H]$^+$), 380,08 /380,20
Compound 4	3132 (N-H s.b.); 3020, 2978 (aromatic C-H s.b.); 2951 (aliphatic C-H s.b.); 1705, 1651 (C=O s.b.); 1620, 1608 (C=N s.b., C=C s.b.)	4.53 (d, 2H, J=5.2 Hz ,N-CH_2-CH-); 5.24 (d, 2H, J=12.8 Hz, -CH=CH_2); 5.96 (m, 1H, CH_2-CH=CH_2); 7.26 – 7.92 (m, 10H, Ar-*H*, =C*H*-Ar); 11.26 (s, 1H, N*H*-N)	APCI$^+$ ([M+H]$^+$), 398,07 / 398,15
Compound 5	3221 (N-H s.b.); 3070 (aromatic C-H s.b.); 2939 (aliphatic C-H s.b.); 1705, 1654 (C=O s.b.); 1600, 1577 (C=N s.b., C=C s.b.)	3.74 (s, 3H, Ar-(5)OCH_3); 3.96 (s, 3H, Ar-(2)OCH_3); 4.59 (d, 2H, -CH_2-CH-); 5.31 (d, 2H, J=16 Hz, -CH=CH_2); 6.02 (t, 1H, CH_2-CH=CH_2); 7.04 – 7.98 (m, 10H, Ar-*H*, =C*H*-Ar); 11.28 (s, 1H, N*H*-N).	APCI$^+$ ([M+H]$^+$), 424,13 / 424,20
Compound 6	3213 (N-H s.b.); 3062, 3032 (aromatic C-H s.b.); 2943 (aliphatic C-H s.b.); 1712, 1647 (C=O s.b.); 1597, 1577, 1481 (N-H b.b., C=N s.b., C=C s.b.)	5.12 (s, 2H, CH_2-Ar); 7.32 – 7.91 (m, 15H, =C*H*-Ar, Ar-*H*); 11.29 (s, 1H, N*H*-N).	APCI$^+$ ([M+H]$^+$), 432,11 / 432,20
Compound 7	3155 (N-H s.b.); 3059, 3028 (aromatic C-H s.b.); 2981, 2943 (aliphatic C-H s.b.); 1743, 1705 (C=O s.b.); 1651, 1612, 1600 (C=N s.b., C=C s.b.)	2.43 (s, 3H, Ar-CH_3); 3.18 (t, 2H, CH_2-Ar); 4.21 (s, 2H, N-CH_2); 7.31 – 7.04 (m, 15H, =C*H*-Ar, Ar-*H*); 11.38 (s, 1H, N*H*-N).	APCI$^+$ ([M-]), 441,15 / 440,25
Compound 8	3109 (N-H s.b.); 3039 (aromatic C-H s.b.); 2954, 2939 (aliphatic C-H s.b.); 2831 (O-CH3 s.b.); 1697 (C=O s.b.); 1620, 1573, 1496 (C=N s.b., C=C s.b., N-H b.b.)	0.92 (t, 3H, J_1= 7.24 Hz, J_2= 7.32 Hz, CH_2-CH_3); 1.75 (q, 2H, CH_2-CH_3); 3.73 (s, 3H, Ar-(5)OCH_3); 3.86 (t, 5H, Ar-(2)OCH_3 and N-CH_2-CH_3); 6.96 (s, 1H, arylidene H4); 7.09 (s, 2H, arylidene H3, H6); 7.78 (d, 2H, J=4.56 Hz, pyridine H3, H5); 7.89 (s, 1H, =C*H*-Ar); 8.77 (d, 2H, J=4.6 Hz, pyridine H2, H6); 11.48 (s, 1H, N*H*-N).	APCI$^+$ ([M+H]$^+$), 427,14 / 427,25
Compound 9	3209 (N-H s.b.); 3059, 3032 (aromatic C-H s.b.); 2970, 2935 (aliphatic C-H s.b.); 2839 (O-CH3 s.b.); 1701, 1654 (C=O s.b.); 1612, 1593 (C=N s.b., C=C s.b.)	3,89 (s, 3H, Ar-OCH_3); 4.52 (s, 2H, N-CH_2-CH-); 5.22 (d, 2H, J=12 Hz, -CH=CH_2); 5.96 (m, 1H, CH_2-CH=CH_2); 7.08 – 7.97 (m, 7H, Ar-*H*, pyridine H3, H5, =C*H*-Ar); 8.77 (d, 2H, J=3.2 Hz, pyridine H2, H6); 11.51 (s, 1H, N*H*-N).	APCI$^-$ ([M-H]$^-$), 393,10 /393,20
Compound 10	3086 (N-H s.b.); 3043, 3012 (aromatic C-H s.b.); 2931 (aliphatic C-H s.b.); 1705 (C=O s.b.); 1616, 1577 (C=N s.b., C=C s.b.)	4.53 (s, 2H, N-CH_2-CH-); 5.26 (t, 2H, -CH=CH_2); 5.96 (m, 1H, CH_2-CH=CH_2); 7.37 – 7.74 (m, 8H, Ar-*H*, pyridine H3, H5, =C*H*-Ar); 8.73 (d, 2H, J=4.52 Hz, pyridine H2, H6); 11.52 (s, 1H, N*H*-N).	APCI$^-$ ([M-H]$^-$), 415,04 /415,15
Compound 11	3062 (N-H s.b.); 3035 (aromatic C-H s.b.); 2981, 2931 (aliphatic C-H s.b.); 1697 (C=O s.b.); 1612, 1573 (C=N s.b., C=C s.b.)	5.12 (s, 2H, CH_2-Ar); 7.33 (m, 11H, Ar-*H*, pyridine H3, H5); 7.95 (s, 1H, =C*H*-Ar); 8.77 (d, 2H, J=4.04 Hz, pyridine H2, H6); 11.59 (s,1H, N*H*-N).	APCI$^-$ ([M-H]$^-$), 447,06 /447,15
Compound 12	3151 (N-H s.b.); 3078, 3039 (aromatic C-H s.b.); 2931 (aliphatic C-H s.b.); 2843 (O-CH3 s.b.); 1697 (C=O s.b.); 1612, 1573 (C=N s.b., C=C s.b.)	3.89 (s, 3H, Ar-OCH_3); 5.09 (s, 2H, CH_2-Ar); 7.12-7.52 (m, 9H, Ar-*H*); 7.82 (d, 2H, J=5.64 Hz, pyridine H3, H5); 7.89 (s, 1H, =C*H*-Ar); 8.64 (d, 2H, J=4.48 Hz, pyridine H2, H6). (N-H proton was exchanged with DMSO deuterium.).	APCI$^-$ ([M-H]$^-$), 443,11 /443,20
Compound 13	3186 (N-H s.b.); 3055, 2970 (aromatic C-H s.b.); 2916, 2862 (aliphatic C-H s.b.); 1705 (C=O s.b.); 1643, 1589 (C=N s.b., C=C s.b.)	5.12 (s, 2H, -CH_2-Ar); 7.27-7.68 (m, 10H, Ar-*H*, =C*H*-Ar); 7.86 (d, J=5.6 Hz, pyridine H3, H5); 8.51 (d, 2H, J=5.56 Hz, pyridine H2, H6); (N-H proton was exchanged with DMSO deuterium).	APCI$^-$ ([M-H]$^-$), 447,06 /447,15
Compound 14	3074 (N-H s.b.); 3032 (aromatic C-H s.b.); 2931 (aliphatic C-H s.b.); 2831 (O-CH3 s.b.); 1701 (C=O s.b.); 1616, 1573 (C=N s.b., C=C s.b.)	3.80 (s, 3H, Ar-OCH_3); 5.12 (s, 2H, -CH_2-Ar); 7.06-7.80 (m, 12H, Ar-*H*, pyridine H3, H5, =CH-Ar); 8.77 (s, 2H, pyridine H2, H6), 11.57 (1H, s, N*H*-N).	APCI$^+$ ([M+H]$^+$), 445,12 / 445,20
Compound 15	3078 (N-H s.b.); 3970 (aromatic C-H s.b.); 2908 (aliphatic C-H s.b.); 2862 (O-CH3 s.b.); 1697 (C=O s.b.); 1604, 1589 (C=N s.b., C=C s.b.)	3.73 (s, 3H, Ar-(5)OCH_3); 3.79 (s, 3H, Ar-(2)OCH_3); 5.10 (s, 2H, CH_2-Ar); 6.97 (s, 1H, arylidene H4); 7.09 (s, 2H, arylidene H3-H6); 7.31-7.45 (m, 5H, Ar-*H*); 7.79 (d, 2H, J=4.24 Hz, pyridine H3, H5); 7.92 (s, 1H, =C*H*-Ar); 8.77 (d, 2H, J=4.76 Hz, pyridine H2, H6); 11.54 (s, 1H, N*H*-N).	APCI$^-$ ([M-H]$^-$), 473,12 /473,25
Compound 16	3213 (N-H s.b.); 3082, 3047 (aromatic C-H s.b.); 2989, 2947 (aliphatic C-H s.b.); 2827 (O-CH3 s.b.); 1712, 1651 (C=O s.b.); 1608, 1593 (C=N s.b., C=C s.b.)	3.07 (s, 2H, CH_2-Ar); 3.74 (s, 3H, Ar-(5)OCH_3); 3.83 (s, 3H, Ar-(2)OCH_3); 4.12 (s, 2H, N-CH_2); 6.95 (s, 1H, arylidene H4); 7.09 (s, 2H, arylidene H3-H6); 7.23-7.31 (d, 5H, Ar-*H*); 7.82 (d, 3H, pyridine H3, H5, =C*H*-Ar); 8.79 (s, 2H, pyridine H2, H6); 11.57 (s, 1H, N*H*-N).	APCI$^-$ ([M-H]$^-$), 487,14 /487,20
Compound 17	3190 (N-H s.b.); 3043, 2989 (aromatic C-H s.b.); 2954, 2873 (aliphatic C-H s.b.); 2835 (O-CH3 s.b.); 1697, 1643 (C=O s.b.); 1608, 1589 (C=N s.b., C=C s.b.)	0.93 (t, 3H, -CH_2-CH_2-CH_3); 1.75 (m, 2H, -CH_2-CH_2-CH_3); 3.90 (d, 5H, Ar-OCH_3, N-CH_2-CH_2-CH_3); 7.10-7.58 (m, 5H, Ar-*H*, =C*H*-Ar); 7.97 (s, 1H, pyridine H5); 8.23 (d, 1H, J=3.6 Hz, pyridine H4); 8.77 (s, 1H, pyridine H6); 9.04 (s, 1H, pyridine H2); 11.39 (1H, s, N*H*-N).	APCI$^-$ ([M-H]$^-$), 395,11 /395,20
Compound 18	3201 (N-H s.b.); 3062 (aromatic C-H s.b.); 2954 (aliphatic C-H s.b.); 2877 (O-CH3 s.b.); 1697 (C=O s.b.); 1643, 1597 (C=N s.b., C=C s.b.)	0.93 (t, 3H, J_1= 6.64 Hz, J_2= 6.88 Hz, -CH_2-CH_2-CH_3); 1.76 (d, 2H, J=6.84 Hz, -CH_2-CH_2-CH_3); 3.84 (d, 5H, Ar-OCH_3, N-CH_2-CH_3); 7.05-7.58(m, 5H, Ar-*H*, =C*H*-Ar); 7.76 (s, 1H, pyridine H5); 8.24 (d, 1H, J=6.88 Hz, pyridine H4); 8.78 (s, 1H, pyridine H6); 9.05 (s, 1H, pyridine H2); 11.42 (1H, s, N*H*-N).	APCI$^-$ ([M-H]$^-$), 395,11 /395,20
Compound 19	3209 (N-H s.b.); 3097, 3055 (aromatic C-H s.b.); 2935 (aliphatic C-H s.b.); 2839 (O-CH3 s.b.); 1705 (C=O s.b.); 1647, 1589 (C=N s.b., C=C s.b.)	3.90 (s, 3H, Ar-OCH_3); 5.10 (s, 2H, N-CH_2); 7.09-7.58 (m, 10H, Ar-*H*, =C*H*-Ar); 8.00 (s, 1H, pyridine H5); 8.23 (d, 1H, J=6.84 Hz, pyridine H4); 8.76 (d, 1H, J=3.04 Hz, pyridine H6); 9.04 (s, 1H, pyridine H2); 11.43 (1*H*, s, N*H*-N).	APCI$^-$ ([M-H]$^-$), 443,13 /443,20
Compound 20	3066 (N-H s.b.); 3020 (aromatic C-H s.b.); 2870, 2781 (aliphatic C-H s.b.); 1716 (C=O s.b.); 1670, 1597 (C=N s.b., C=C s.b.)	5.12 (s, 2H, N-CH_2-Ar); 7.31-7.81 (m, 11H, Ar-*H*, =C*H*-Ar, pyridine H5); 8.24 (d, 1H, J=6.80 Hz, pyridine H4); 8.76 (d, 1H, J=2.92 Hz, pyridine H6); 9.06 (s, 1H, pyridine H2); 11.49 (1H, s, N*H*-N).	APCI$^-$ ([M-H]$^-$), 447,06 /447,15
Compound 21	3201 (N-H s.b.); 3086 (aromatic C-H s.b.); 3028 (aliphatic C-H s.b.); 1708 (C=O s.b.); 1654, 1616 (C=N s.b., C=C s.b.)	3.10 (s, 2H, CH_2-Ar); 4.13 (s, 2H, N-CH_2); 7.24-7.82 (m, 11H, Ar-*H*, =C*H*-Ar, pyridine H5); 8.25 (d, 1H, J=7.2 Hz, pyridine H4); 8.77 (d, 1H, pyridine H6); 9.07 (s, 1H, pyridine H2); 11.52 (1H, s, N*H*-N).	APCI$^-$ ([M+H]$^-$), 507,04 /507,10
Compound 22	3116 (N-H s.b.); 3078, 3028 (aromatic C-H s.b.); 2939, 2889 (aliphatic C-H s.b.); 2839 (O-CH3 s.b.); 1701, 1651 (C=O s.b.); 1612, 1593 (C=N s.b., C=C s.b.)	3.09 (s, 2H, CH_2-Ar); 3.89 (s, 3H, Ar-OCH_3); 4.12 (s, 2H, N-CH_2); 7.09-7.58 (m, 10H, Ar-*H*, =C*H*-Ar); 7.88 (s, 1H, pyridine H5); 8.26 (d, 1H, J=7.36 Hz, pyridine H4); 8.78 (d, 1H, J=3.64 Hz, pyridine H6); 9.08 (s, 1H, pyridine H2); 11.47 (1H, s, N*H*-N).	APCI$^-$ ([M-H]$^-$), 457,13 /457,25

	X	Y	R	R_1	R_2	R_3	R_4	R_5
Compound 1	C	C	Ethyl	H	H	H	H	H
Compound 2	C	C	Ethyl	H	F	H	H	H
Compound 3	C	C	Allyl	F	H	H	H	H
Compound 4	C	C	Allyl	H	H	Cl	H	H
Compound 5	C	C	Allyl	-OCH_3	H	H	-OCH_3	H
Compound 6	C	C	Benzyl	F	H	H	H	H
Compound 7	C	C	Phenethyl	H	-CH_3	H	H	H
Compound 8	N	C	Propyl	-OCH_3	H	H	-OCH_3	H
Compound 9	N	C	Allyl	-OCH_3	H	H	H	H
Compound 10	N	C	Allyl	Cl	H	H	H	F
Compound 11	N	C	Benzyl	Cl	H	H	H	H
Compound 12	N	C	Benzyl	-OCH_3	H	H	H	H
Compound 13	N	C	Benzyl	H	Cl	H	H	H
Compound 14	N	C	Benzyl	H	-OCH_3	H	H	H
Compound 15	N	C	Benzyl	-OCH_3	H	H	-OCH_3	H
Compound 16	N	C	Phenethyl	-OCH_3	H	H	-OCH_3	H
Compound 17	C	N	Propyl	-OCH_3	H	H	H	H
Compound 18	C	N	Propyl	H	-OCH_3	H	H	H
Compound 19	C	N	Benzyl	-OCH_3	H	H	H	H
Compound 20	C	N	Benzyl	H	Cl	H	H	H
Compound 21	C	N	Phenethyl	Br	H	H	H	H
Compound 22	C	N	Phenethyl	-OCH_3	H	H	H	H

RESULTS

Following our molecular modelling studies, N-substituted thiazolidin-4-one compounds bearing arylidene groups from a database containing approximately 15,000 compounds were proposed for synthesis. These compounds were synthesized and elucidated by IR, 1H-NMR and mass spectral techniques. Impurity controls were performed by HPLC and TLC methods.

CONCLUSION

We selected several new compounds for sythesis using molecular modelling studies. Subsequently 22 new N-substituted thiazolidin-4-one compounds bearing the arylidene group were synthesized and their structures were confirmed by IR, NMR and mass spectroscopy after purity checks.

ACKNOWLEDGEMENT

Presenter is supported by 2211-A PhD Scholarship Program of TÜBİTAK and 100/2000 YÖK PhD Scholarship Program. We would like to thank both institutions for their support.

REFERENCES

1. Rozman et al (2017). Drug Discov Today, 22(3):492-502.
2. Chetty et al (2017). Bioorg Med Chem Lett, 27(3):370-386.
3. Borsari et al (2017). Drug Discov Today, 22(3):576-584.
4. Tatar et al (2016). Biol Pharm Bull, 39(4):502-15.
5. Tatar et al (2010). International Journal of Drug Design and Discovery, 1:19-32.